Quaternary Research 83 (2015) 150–165

Contents lists available at ScienceDirect

Quaternary Research

journal homepage: www.elsevier.com/locate/yqres

A soil chronosequence on Lake Mega-Frome beach ridges and its implications for late Quaternary pedogenesis and paleoenvironmental conditions in the drylands of southern Australia

Jan-Hendrik May [a], Stephen G. Wells [b], Timothy J. Cohen [a], Samuel K. Marx [a], Gerald C. Nanson [a], Sophie E. Baker [b]

[a] GeoQuest Research Centre, School of Earth and Environmental Sciences, University of Wollongong, Wollongong, 2522 NSW, Australia
[b] Desert Research Institute, Nevada System of Higher Education, Reno, NV 89512, USA

ARTICLE INFO

Article history:
Received 1 July 2014
Available online 9 December 2014

Keywords:
Beach ridges
Soil formation
Chronosequence
late Quaternary
Desert pavement
Eolian dust
Paleoenvironments

ABSTRACT

The terminal lake systems of central Australia are key sites for the reconstruction of late Quaternary paleoenvironments. Paleoshoreline deposits around these lakes reflect repeated lake filling episodes and such landforms have enabled the establishment of a luminescence-based chronology for filling events in previous studies. Here we present a detailed documentation of the morphology and chemistry of soils developed in four well-preserved beach ridges of late Pleistocene and mid-to-late Holocene age at Lake Callabonna to assess changes in dominant pedogenic processes. All soil profiles contain evidence for the incorporation of eolian-derived material, likely via the formation of desert pavements and vesicular horizons, and limited illuviation due to generally shallow wetting fronts. Even though soil properties in the four studied profiles also provide examples of parent material influence or site-specific processes related to the geomorphic setting, there is an overall trend of increasing enrichment of eolian-derived material since at least ~33 ka. Compared to the Holocene profiles, the derived average accumulation rates for the late Pleistocene profiles are significantly lower and may suggest that soils record important regional changes in paleoenvironments and dust dynamics related to shifts in the Southern Hemisphere westerlies.

Introduction

Lakes and lake sediments are among the most commonly used archives for the reconstruction of late Quaternary terrestrial paleoenvironments and hydrology. In arid southern Central Australia, the large terminal lake systems of Lake Eyre, Lake Frome, Lake Callabonna, Lake Blanche, and Lake Gregory, have long been considered key sites for paleoenvironmental studies (Magee et al., 1995; Nanson and Price, 1998). At Lake Frome, a number of studies utilized lake sediments (Draper and Jensen, 1976; Bowler et al., 1986; Ullman and Collerson, 1994) and pollen or microfaunal remains (Singh, 1981; Singh and Luly, 1991; Luly, 2001; De Deckker et al., 2011) to develop a paleoclimatic framework for the region. More recent efforts have predominantly focused on the analysis of paleoshoreline deposits (Nanson et al., 1998; Cohen et al., 2011, 2012a, 2012b). Their detailed topographic survey (DeVogel et al., 2004; Leon and Cohen, 2012) has placed new constraints on variations in lake levels and water volume. Recent advances in dating techniques have enabled a significantly improved understanding of the depositional ages associated with the individual beach ridges and shorelines, and thus the timing of late Quaternary lake stands around Lake Frome and Callabonna (Cohen et al., 2011, 2012a, 2012b; Gliganic et al., 2014). Paleoshorelines, and particularly the soils formed within successively older beach ridges (i.e. soil chronosequence) thus provide powerful tools to examine the influence of time on soil development, and explore the effects of changes in soil-forming factors such as climate or vegetation cover on soil properties, pedogenic processes and evolution (Johnson et al., 1990; Birkeland, 1992; Huggett, 1998; Dixon, 2013; Schmid, 2013). In this paper, we present the first detailed assessment of soil properties related to a recently dated chronosequence composed of four late Pleistocene to late Holocene beach ridges at Lake Callabonna in order to assess the key processes influencing soil development as well as the evolution of these soils which developed along the margins of these late Quaternary mega-lakes. Our study thus directly endeavors (i) to improve our understanding of pedogenic processes in the arid environment of southern Australia; (ii) to assess the relative role of time versus environmental change on late Quaternary soils over the past ~33 ka; and (iii) to evaluate the potential use of soils around Lake Mega-Frome as complementary archives capable of recording paleoenvironmental conditions over timescales longer than covered by short-lived lake stands (McFadden et al., 1992; Fedoroff and Courty, 1999; Barrett, 2001).

http://dx.doi.org/10.1016/j.yqres.2014.11.002
0033-5894/

Study area

Physical and geological setting

Lakes Frome, Callabonna, Blanche, and Gregory form an arcuate chain of playa lakes around the northern and north-eastern Flinders Ranges in South Australia (Fig. 1). While all four lakes receive highly intermittent inflow from the west and southwest via creeks sourced in the ranges, Lake Blanche is also fed from the north by the Strzelecki Creek, which is an overflow channel of the Cooper Creek and is active only during the largest recorded floods (Nanson et al., 1998). The study region has an arid to semi-arid climate with a mean annual precipitation of ~150–200 mm around the lakes but as high as 300–400 mm in the Flinders Ranges (Schwerdtfeger and Curran, 1996). Most of the rain falls during summer via incursions of tropical moisture from the north, even though the Southern Westerlies still contribute ~20–40% of the annual precipitation (Cohen et al., 2012b). Mean wind directions are mainly southerly and southwesterly (Sprigg, 1982). In contrast, dust storms are associated with southerly, westerly or northerly winds resulting from the passage of frontal systems (Sprigg, 1982) and activate sediment from variable source areas (Bullard et al., 2008). Mean temperatures vary from ~15°C in winter to ~30°C in summer, leading to considerably high potential evaporation rates of ~2000 mm/yr (Schwerdtfeger and Curran, 1996). Consequently, the vegetation cover is dominated by xerophytic grasses, shrubs and bushes, with trees mostly limited to the water courses or the higher slopes of the Flinders Ranges. In the vicinity of the playa lakes, vegetation is characterized by increasingly salt tolerating species (Gell and Bickford, 1996). Where the land surface is covered with stone (desert) pavements (e.g. alluvial fans, shorelines) vegetation cover can be almost completely absent. The alluvial fans around the southwestern and western lake margins are built from coarse-grained fluvial–alluvial deposits. Clast lithologies reflect a provenance in the highly folded Flinders Ranges where Paleoproterozoic metasediments, Mesoproterozoic granitoids and volcanics, and Neoproterozoic sedimentary rocks all overly a crystalline basement (Sheard, 2009). Around their eastern and north-eastern margins, lakes Frome and Callabonna are bounded by the extensive dune field of the Strzelecki Desert which consists of a complex array of longitudinal dunes as well as transverse and source-bordering dunes (Fitzsimmons, 2007; Fitzsimmons et al., 2009).

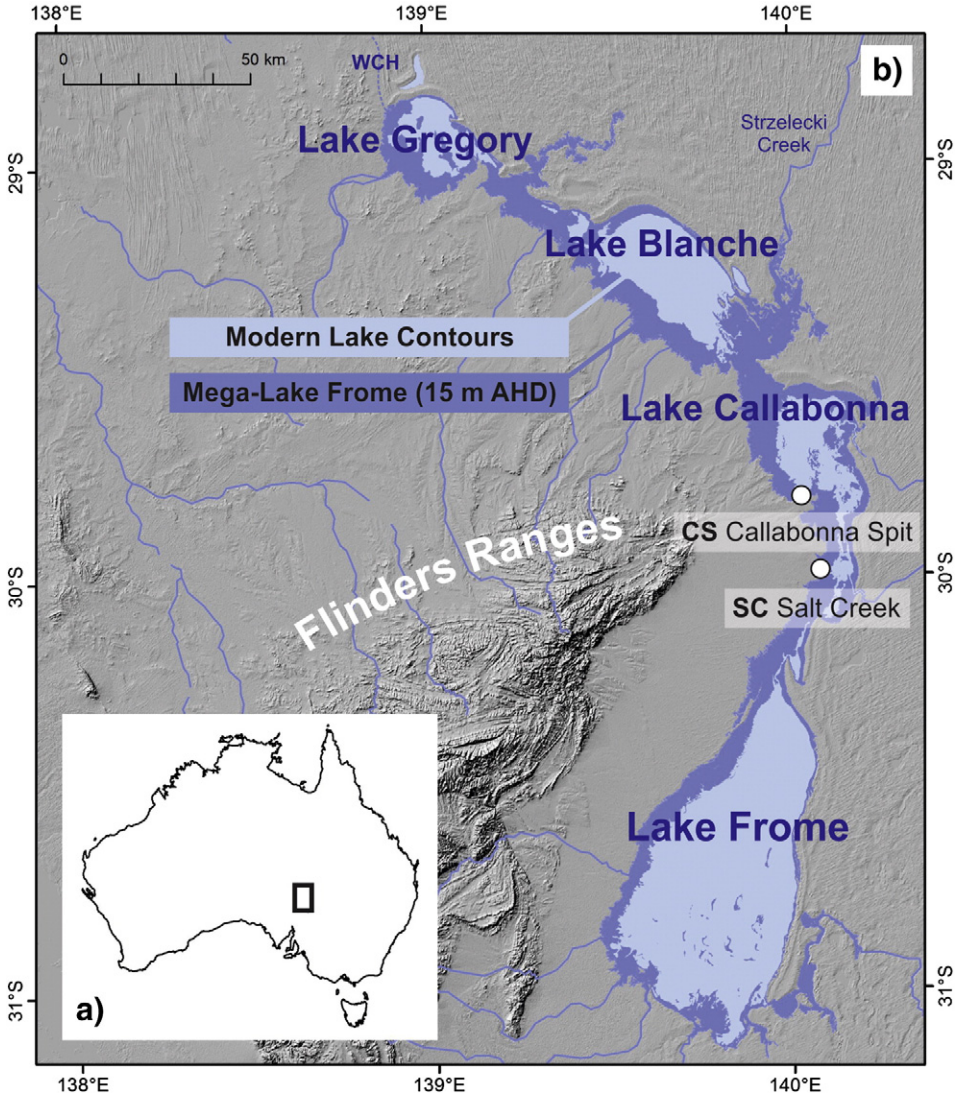

Figure 1. Regional setting of study area. (a) Location in Australia. (b) Geographic setting of studied shoreline sites, and their location with regard to Lake Frome, Callabonna, Blanche and Gregory (light blue) and maximum extent of pre 45 ka Lake Mega-Frome (dark blue) as controlled by the Warrawoocara sill (WCH) at ~15–16 m AHD (Australian Height Datum) (Nanson et al., 1998; Cohen et al., 2012b).

https://doi.org/10.1016/j.yqres.2014.11.002 Published online by Cambridge University Press

Quaternary stratigraphy and shorelines at Salt Creek and Callabonna Spit

Late Quaternary deposits flanking Lakes Frome and Callabonna are mapped as shoreline sediments or paleoshoreline deposits of the Pleistocene Coomb Spring Formation or Holocene Coonarbine Formation (Callen and Tedford, 1976; Sheard, 2009). These paleoshorelines, referred to as beach ridges in the following, are discontinuous elongate to sinuous landforms extending up to several km in length around the lake margin, and where exposed in channel margins or trenches exhibit a stacked stratigraphic sequence that reflects vertical accretion during extended or repeated lake stands (Cohen et al., 2012b). The most distinct beach ridges occupy the western and southwestern margins of Lake Callabonna (Figs. 2, 3) and Lake Frome. Their morphology and preservation vary from more sinuous, narrow lower and younger ridges to the broad, subdued and partially dissected topography of the older shorelines (Figs. 3a, b). At ~15–16 m AHD (Australian Height Datum) the highest ridge is equivalent to the lake highstand, reflecting the topographic elevation of the overflow channel to Lake Eyre, the Warrawoocara channel (Fig. 1b; Nanson et al., 1998). Corresponding water depths > 15 m at Lake Frome and Callabonna were reached at least three times between ~110 and 45 ka (Cohen et al., 2011, 2012b). Below this elevation three major lower beach ridges correspond to successively smaller lake stands during Marine Oxygen Isotope Stage (MIS) 3 (~10–12 m), during the transition from the Last Glacial Maximum to the early deglacial period (~7 m), and in the mid-Holocene (~5 m) (Cohen et al., 2012b), when the four lake basins of Lake Frome, Callabonna, Blanche and Gregory connected to form the continuous body of water defined here as Lake Mega-Frome (Callen and Tedford, 1976; Cohen et al., 2011). Minor late Holocene lake stands at 3.5–2.7 and 1 ka are recorded at Lake Callabonna in beach ridges below ~4 m AHD (Gliganic et al., 2014).

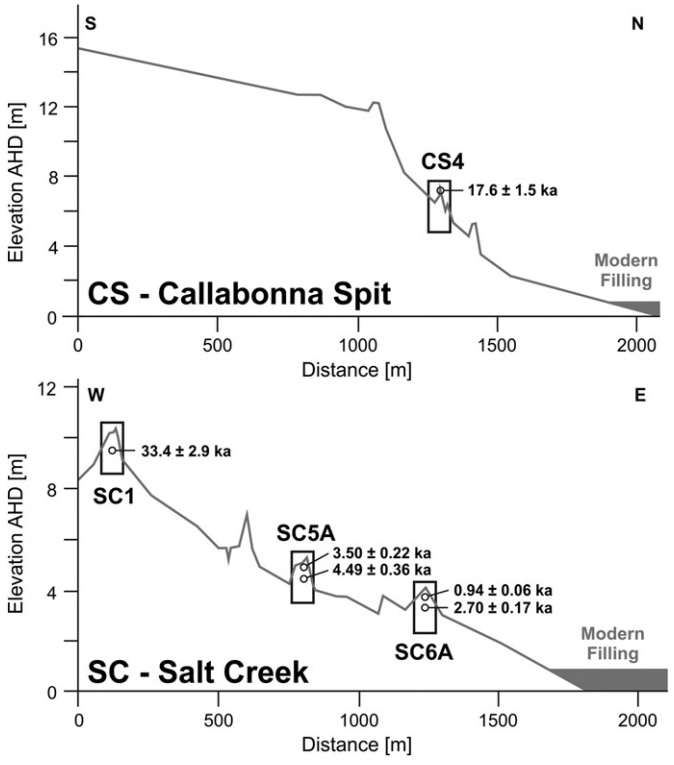

Figure 2. Topographic transects across Late Pleistocene to Holocene beach ridge complexes at Callabonna Spit (CS) and Salt Creek (SC) study sites on Lake Callabonna. Boxes mark the location of sampled pits/trenches.

Methodology

Four successively older and higher beach ridges were selected at the two localities of Salt Creek (SC) and Callabonna Spit (CS) along the southwestern shore of Lake Callabonna (Table 1, Figs. 1, 2). The chronology for the four studied beach ridges is based on a combination of single-grain OSL and ^{14}C ages presented elsewhere (Cohen et al., 2012a, 2012b; Gliganic et al., 2014) and is broadly illustrated in Fig. 2 with details summarized in Table 1. On the crest of each of these beach ridges, which represents the most stable part of these landforms, a ~1.5 m by 3 m wide pit of 2–3 m depth was trenched with a mechanical excavator. Descriptions of lithology and sedimentary structures as well as the interpretations of stratigraphy were adapted from Cohen et al. (2012a, 2012b). In each of these pits, soil horizons were described in the field based upon their major macroscopically visible morphological characteristics (Table 2) according to Schoeneberger et al. (2002). A modified Horizon Development Index (HDI) and a Profile Development Index (PDI) were then calculated for each of the horizons and profiles, respectively, based on quantification of texture, structure, clay films (frequency and location), as well as consistency (plasticity and stickiness) (Harden, 1982). Also, the Hurst-Index was calculated for each horizon from dry Munsell colors and used as a measure of redness, with decreasing index values indicating increasing redness (Hurst, 1977). Bulk samples of up to ~300 g were taken per soil horizon in sealed sample bags for laboratory analysis at the Desert Research Institute (DRI) where field moisture content was determined (weight loss after air drying at room temperature). Gravel content was determined by sieving through a 2 mm mesh sieve using a mechanical shaker for 5 min. All subsequent analyses were performed on the fine earth (<2 mm) fraction, with one in every ten samples analyzed in duplicate.

Gypsum content was measured using the thermogravimetric method (Lebrón et al., 2009), which exploits the gypsum–bassanite phase change. The percent weight calcium carbonate in each sample was determined using the pressure calcimeter method (Sherrod et al., 2002) on a ground subsample. Total soluble salt content was estimated by measuring the electrical conductivity of an aqueous soil extract using a standard conductivity meter (Rhoades et al., 1996). Soil pH was measured using a standard pH meter on a 1:1 soil-aqueous matrix suspension made using a 0.01 M calcium chloride ($CaCl_2$) solution (Thomas et al., 1996). The iron oxide content of samples was determined by measuring the Fe content of two soil extracts per sample using Atomic Absorption Spectrometry. Respectively, the two extracts were made using: (i) the dithionite–citrate method to extract Fe bound in non-crystalline and crystalline Fe oxides (also referred to as total 'free' or 'pedogenic' iron oxides Fe_d; Cornell and Schwertmann, 2006); and (ii) the acid hydroxylamine method to extract Fe from non-crystalline and poorly crystalline iron oxides (Fe_o). The latter procedure is similar to the more commonly used acid ammonium oxalate method but is preferable because it does not have to be performed in the dark (Ross and Wang, 1993). Grain size distribution was determined using a combination of sieving and laser diffraction techniques (Gee et al., 1986). Samples containing >2% carbonate were pretreated with glacial acetic acid prior to analysis to break up aggregates bound by carbonate. A split of the fine earth (<2 mm) fraction was dispersed (shaken overnight in an aqueous surfactant solution of 0.01% sodium metaphosphate) and then wet sieved to remove the sand fraction. The fine fraction was subsequently analyzed by laser diffraction using a Micromeritics Saturn Digisizer® (Micromeritics, Inc., Norcross, GA) within which the sample was dispersed using ultra-sonication in the surfactant solution and circulated through the path of the laser-light beam. Exclusion of the sand fraction from the laser analysis was chosen because the Saturn Digisizer instrument produces more consistent results when the total particle size range of the sample is relatively small, and because grains larger than ~500 μm cannot be suspended effectively within the instrument. Combining the gravimetric sieve data and volume-based laser diffraction data into a single particle size distribution requires the assumption that all particle size fractions have a similar density. To

https://doi.org/10.1016/j.yqres.2014.11.002 Published online by Cambridge University Press

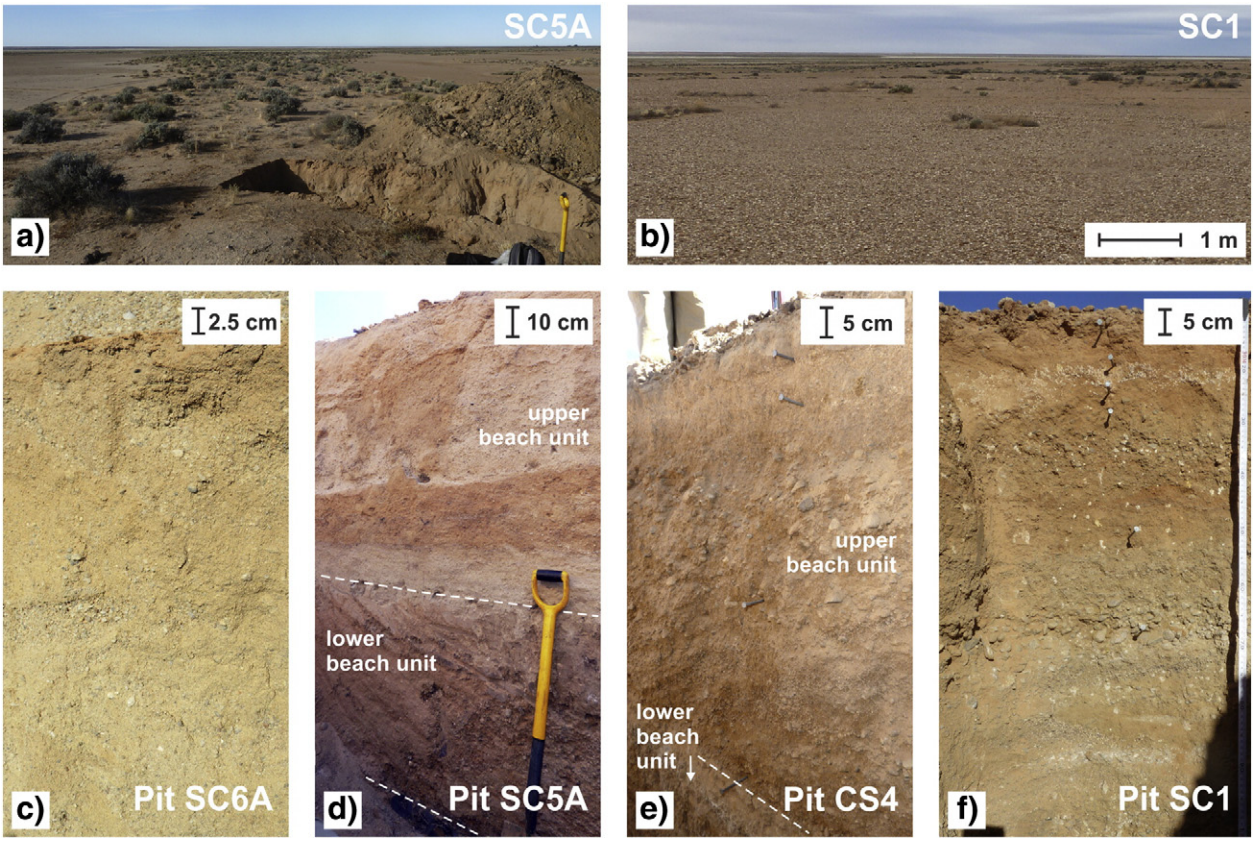

Figure 3. Field photos of beach ridges at Salt Creek (SC) showing the differences in width, vegetation cover and surface armoring between the mid-to-late Holocene ridge at SC5A (a) and the MIS3 ridge at SC1 (b). Close-ups of soil pits (c–f) at Salt Creek and Callabonna Spit (CS). Note the tendency of overall reddening from youngest (c) to oldest (f) soil profile, as well as the marked white gypsum specs in the oldest ridge Pit SC1.

facilitate comparison between the profiles, weight percentages of silt, clay, $CaCO_3$, gypsum, soluble salts, Fe_d, and Fe_o were converted to total accumulation weight per horizon and m^2, using an approach for estimating soil bulk density based on matrical grain size data and bulk gravel content (Saxton and Rawls, 2006). Any difference between the actual and estimated bulk density will influence soil accumulation rates, however the main focus on the paper is on relative changes between the soil pits, and these are not affected by differences in actual and estimated bulk density. These horizon averages were then summed over the whole soil profile (i.e. pit depth), and the depth of the stratigraphically uniform beach sands and gravels (i.e. soil depth), respectively. Finally, the values for total soil profile accumulation weight per m^2 were divided by soil ages derived from existing chronology to estimate time-averaged accumulation rates expressed in $g/m^2/yr$.

Results

Field and laboratory data for soil profiles described on the Lake Frome and Lake Callabonna shorelines (Fig. 3) are summarized in Tables 2 and 3. These show increasing morphological and textural development in progressively older beach ridges. The depths of the individual soil horizons, in relation to beach ridge stratigraphy, and down-profile variation in textural and key chemical properties are illustrated in Fig. 4. This forms the basis for elucidating the changes in soil morphology and chemistry from the youngest to the oldest studied ridge.

Topography, sediments, and chronostratigraphy

The youngest Holocene beach ridge and shoreface at Salt Creek form a ~100–150 m wide laterally extensive and morphological complex (at ~4.0 ± 0.2 m AHD) feature (Figs. 2, 3c, Table 1; Cohen et al., 2012a). Two stratigraphic units composed of partially landward dipping high-energy beach sands and gravel were observed in Pit SC6A (Figs. 4). The lower of the two units has been dated to ~2.7 ka. The upper unit consists of 60 cm of gravelly sand that was deposited during the Medieval Climate Anomaly ~0.94 ka (Cohen et al., 2012a). The soil profile on this beach ridge (Pit SC6A, Tables 2, 3, Figs. 3c, 4) was only developed in the upper stratigraphic unit, and thus the field and lab data reflect pedogenesis over approximately the last millennium.

Table 1
Location and chronological details of the four studied soil pits (* Ages are in ka for OSL, and cal ka BP for ^{14}C; errors are 1σ for OSL and 2σ for ^{14}C).

Pit	Latitude	Longitude	Elevation	Age*	Position in Beach Ridge	Method	Reference
SC 1	−29.9396°	140.1130°	~10.4 m AHD	33.4 ± 2.9	Lower unit	SG OSL	Cohen et al. (2012b)
CS 4	−29.8048°	140.0811°	~7.2 m AHD	17.6 ± 1.5	Upper unit	SG OSL	Cohen et al. (2012b)
SC 5A	−29.9403°	140.1201°	~5.3 m AHD	0.83 ± 0.06	Upper unit	^{14}C	Gliganic et al. (2014)
				3.50 ± 0.22	Upper unit	SG OSL	Gliganic et al. (2014)
				4.49 ± 0.36	Lower unit	SG OSL	Cohen et al. (2012b)
SC 6A	−29.9407°	140.1243°	~4.2 m AHD	0.94 ± 0.06	Upper unit	SG OSL	Cohen et al. (2012a)
				2.70 ± 0.17	Lower unit	SG OSL	Cohen et al. (2012a)

https://doi.org/10.1016/j.yqres.2014.11.002 Published online by Cambridge University Press

The mid-to-late Holocene shoreline at Salt Creek is expressed as a laterally extensive and ~80–100 m wide beach ridge at ~5.3 m AHD (Figs. 2, 3d; Table 1). Similar to the late Holocene beach ridge, it is a composite ridge, i.e. the stratigraphic profile exposed in Pit SC5A exhibits two units of weakly bedded beach sands and gravel resting on older lacustrine deposits (Figs. 3d, 4). Both beach units are separated by a unit of finer, muddy-sandy near-shore deposits. The lower beach sands and lacustrine deposits are characterized by numerous manganese stains, and the boundary between these two stratigraphic units shows cracks that extend into the lacustrine muds which are filled with beach sands. The lower unit has been OSL dated to ~4.5 ka. The upper unit of slightly coarser beach sands and pebbles yielded an OSL age of 3.5 ka (Table 1). An additional radiocarbon age of 0.83 cal ka BP was obtained from a hearth-like feature exposed in the profile at few cm below the surface. The boundary surface between the two stratigraphic units in both the youngest and the late Holocene beach ridges are interpreted to be diastems, or minor depositional breaks, as no soil formation was observed in the lower stratigraphic unit at either location.

Around Lake Callabonna, shorelines corresponding to the transition from the Last Glacial Maximum (LGM) to the deglacial period are either less well developed and/or less preserved than either younger or older shorelines (Cohen et al., 2012b). However at the Callabonna Spit (Fig. 1), the Latest Pleistocene shoreline is expressed by several beach ridges up to 700 m long and ~40 m wide at ~7.2 m AHD. Stratigraphic exposures in Pit CS4 consisted of two successive units composed of near-shore muddy sands with overlying landward-dipping gravelly beach sands (Figs. 3e, 4). An OSL age of 17.6 ka from the upper beach unit indicates a high lake stand with shoreline deposition shortly after the LGM (Cohen et al., 2012b). No ages are available for the lower stratigraphic unit. Of note is a truncated, buried soil at a depth of 145 cm below the surface which displays strongly developed morphological soil properties. This buried soil was not observed in any other exposure in the study area and, unlike the stratigraphic units in the Holocene beach ridges, indicates a prolonged period of subaerial exposure before deposition of the youngest units at this site.

The late Pleistocene shoreline corresponding to MIS 3 is expressed as a comparatively broad (>100 m) low-relief beach ridge complex at ~10 m AHD around Lake Callabonna (Figs. 2, 3b; Cohen et al., 2012b). Pit SC1 is located at the crest of this complex at 10.4 m AHD and exposed ~1 m of beach facies, consisting of poorly sorted gravel overlying landward dipping cross-bedded gravelly sands (Figs. 3f, 4). An OSL age at the base of the beach unit yielded 33.4 ka overlying older fine-grained lacustrine deposits (Cohen et al., 2012b).

Surface properties and stone pavements

All soil profiles have vesicular A (Av) horizons of varying thickness which are typically overlain by a thin veneer of clasts forming stone pavements and recently deposited eolian silty sand (C horizons). The surface of the youngest (~0.94 ka) beach ridge (SC6A) is covered by loose sand and gravel overlying a thin (1.5 cm), platy and vesicular Av horizon characterized by weak polygonal cracking, weakly developed siltans, and incipient stone pavement development. The mid-to-late Holocene beach ridge (SC5A) displays greater surface modification and pedogenic development by comparison. The late Holocene beach ridge is underlain by a weakly developed 3 cm thick vesicular Av horizon which is mantled by a weakly developed, yet more densely packed, stone pavement in comparison to the mid-to-late Holocene beach ridge, (Fig. 4). In contrast to the Holocene beach ridges, the surface and shoreface of the youngest Pleistocene beach ridge (CS4) is mantled by a moderately well-developed gravelly pavement. Loose silty sand occurs in the spaces between, immediately below the pavement clasts above a 5 cm thick Avk horizon as well as along the ped faces, and is referred to as a C horizon given the loose silty sand represents relatively fresh eolian deposits. The surface of the oldest beach ridge (SC1) is almost completely armored by a very well-developed pavement (Fig. 3b), consisting of tightly spaced and well-sorted gravel clasts and fine-grained matrix surrounding them. In both Pleistocene ridges, a 5-cm thick vesicular horizon immediately underlies the pavement.

Soil horizons, texture and morphology

Soil profile thickness in the investigated beach ridges varies between ~67 cm in the youngest beach ridge (SC6A) to >170 cm in the mid-to-late Holocene beach ridge at SC5A. With the exception of the youngest Holocene beach ridge (SC6A), all soil profiles extend across at least one stratigraphic boundary (Fig. 4). This implies landform stabilization (i.e., lake lowering and shoreline abandonment) relatively soon after the deposition of the youngest stratigraphic unit. Below the vesicular Av horizon, all profiles have either cambic (Bw) or weak argillic (Bt) horizons that range from 5 to 60 cm in thickness, but show a trend of increasing complexity in soil morphological observations in the successively older beach ridges (Table 2) and in the degree of differentiation of their horizons (Fig. 4). The soil profile in the youngest ridge (SC6A) consists of a cambic and calcic horizon underlying the vesicular horizon. Similarly, the soil profile described at SC5A consists of a cambic and calcic horizon below the vesicular horizon, but also includes salic (Bz) and silica-enriched (Bq) horizons, and which had developed across two beach units into lacustrine muds. The soil profile near the crest of the broad youngest Pleistocene ridge (CS4) exhibits the most complex sequence of soil horizons including vesicular, cambic, argillic, calcic and salic horizons. By contrast, the soil profile in the oldest investigated beach ridge (SC1) is characterized by a sequence of cambic, salic and calcic horizons below a vesicular horizon.

Textural and grain size properties in all soil profiles varied according to the stratigraphy and properties of the parent material (e.g. the original shoreline deposit). Increased clay and silt content corresponded to lacustrine and near-shore lacustrine sediments (e.g. SC5A, CS4), while a sand content of >80–90% occurs in the high-energy beach sediments. Notwithstanding the generally homogenous sandy parent material of the beach units, there is a clear trend of increased accumulation of fines (clay and silt content) in the Av and Bw horizons showing a gradational decrease down-profile in all the soils analyzed (Fig. 4). In addition, more fines occur in the soils developed in the Pleistocene beach ridge units when compared to the Holocene ones. This difference is also reflected in the detailed macroscopical observations of soil morphology (Table 2) which shows mainly nonsticky and nonplastic consistencies in the Holocene soil profiles and dominantly slightly sticky and plastic consistencies and loamy structures in the Pleistocene profiles. Soil structure appears to exhibit more variability, with single grain to very faint granular structure and some weak crumb structure in the youngest soil profile (SC6A), and subangular blocky to varying degrees of angular blocky structure and weakly developed peds in the mid-to-late Holocene soil profile (SC5A). Similarly, soil structure in the Pleistocene soil profiles (CS4 and SC1) varies down-profile from platy and angular blocky in the Avk horizon, to more granular to single grain and crumby, and angular to subangular blocky in the lower part of the profiles. Also, clay (cutans) and silt (siltans) films were observed in all profiles. In particular, clay films are less developed in the youngest soil profile (SC6A), but more abundant in SC5A where they form well-developed coatings and bridges between the grains in the Av, Bw, and particularly the calcic Bwk horizons. In the Pleistocene profiles, clay films also seem to be best developed in some of the calcic and salic horizons (Bwkz in CS4, Bz–Bzk–Bz in SC1), forming bridge structure between the grains. In contrast to CS4, translocated clay or silt films are nearly absent in the Bw1-3 of SC1 and occur rarely bridge grains in the Bwz1 horizon.

Soil color and redness index

The soil profiles show an overall tendency of reddening with age, from dominantly yellowish-red hues (10YR) younger beach ridge soil,

https://doi.org/10.1016/j.yqres.2014.11.002 Published online by Cambridge University Press

Table 2
Detailed pedon and soil morphological descriptions.

Location and coordinates	Horizon	Depth [cm]	Thickness [cm]	Color dry	Color wet	Texture	Structure	Consistency wet	Clay films	$CaCO_3$	Salts	Pores	Boundary	Comments
Pit SC6A	C	0–1	1	–	–	–	gr	so po	–	–	–	–	–	loose material overlying Av
"Late Holocene" E 415473	Av	1–2.5	1.5	7.5YR 6/4	7.5YR 4/4	LS	1fpl	vss po	vfcobr	n.o.	n.o.	1vf	vaw	very fine weakly developed siltans; polygonal cracking with polygons ~5 cm in diameter
N 6687438 4.2 m AHD	Bw1	2.5–10.5	8	10YR 5/3-4	10YR 4-3/4	S to SL	sg to f-vfgr	so po	n1vfco	n.o.	n.o.	1f tubular, cracks	aw	very fine siltans
	Bw2	10.5–23.5	13	10YR 6/6	10YR 3/4-6	S to SL	sg f-m to 1vfcr	so po	ncobr	n.o.	n.o.	1vf tubular	gw	siltans bridging grains
	Bwk	23.5–49.5	26	10YR 7/4	10YR 5/3	S	sg f-m to 1fcr	so po	v1fco	ve-e, <stage I	n.o.	1vf-f	gw	mottling with colors 10YR 6/6 (15–25%); carbonate = thin discont. Coatings on larger clasts
	Bk	49.5–66.5	17	10YR 7/3	10YR 6/2	S	sg f to 1vffcr	so po	n.o.	es, <stage I	n.o.	1vf	cw	mottling with 10YR 6/6 colors; carbonate = thin discont. Coatings on larger grains
Pit SC5A	Av	0–3	3	7.5YR 6/6	7.5YR 4/6	LS	f-mpl to f-msbk	so po	2dcobr	n.o.	n.o.	1f	aw	mantled with weak stone pavement; vesicles in upper 1 cm, weak vesicular overall
"Mid-Holocene" E 415079	Bw1	3–11	8	7.5YR 6/4-6	7.5YR 4/6	LS	f-c sbk	so po	2fcobr	n.o.	n.o.	1f tubular	cw	siltan bridging present; weak mottling present as lamelli
N 6687201 5.3 m AHD	Bw2	11–32	21	7.5YR 6/4	7.5YR 4/4-6	LS	f-c sbk	so to ss po	2dcobr	n.o.	n.o.	1f tubular-circular	gw	siltan bridging present; mottling = 1–2 mm thick lamellae (little color difference)
	Bwk	32–92	60	7.5YR 6/3-4	7.5YR 4/6	S	sg-msbk	so po	co	n.o.	n.o.	1f	vas	complex mottling with "Bwk fingers": f-m sbk to m pr; so po; 2f tubular–circular; 2 br siltans, 1nco (less colloidal stains); CaCO3 - < stage I, se & 10YR 6/4 dry to 10YR 5/3wet; fingers 10–40 cm apart & 10–40 cm thick, connected to lower unit, fingers thin downward, foreset preserved
	Bqz1	92–105	13	7.5YR 7/6-8	10YR 6-5/4	S	1 m-cabk	so po	nbr	n.o.	<stage I	2 fm circular to tubular	cw	stains and no cutans; clay films in pockets producing mottles; thin discontinuous coatings of salt; prominent cm thick laminations of silica
	Bqz2	105–122	17	7.5YR 6/6	10YR 6/4	S	m-cabk to 1f-mcr	so po	mk-npo-pf	n.o.	<stage I	1-2f-m	vaw	salts as blebs and thin coatings; mottling due to clay bands and manganese coatings and smears
	Bqz3	122–144	22	10YR 7/3	10YR 6/2	SL - SiL	n.a.	vss po	2d	n.o.	stage I	1fpo	cw	siltan bridging; salts occur as blebs; homogeneous color
	2Bzk	144–170	35	10YR 7/3	10YR 5/4	–	1f-mabk	vs p	1n-po	e, stage I	stage I	2f-c, cracks	cw	clay films as coatings; carbonate as nodules and blebs; manganese stains <10% bands 1 mm to 1 cm thick; lake sediments below are turbated & cracked in a

(continued on next page)

Table 2 *(continued)*

Location and coordinates	Horizon	Depth [cm]	Thickness [cm]	Color dry	Color wet	Texture	Structure	Consistency wet	Clay films	$CaCO_3$	Salts	Pores	Boundary	Comments
														mixing layer
	3Bzk	179–215+	36+	10YR 7-6/3 - 7.5YR 6/8	10YR 7/2 - 10YR 6/6	–	1 sg to f-mabk	n.a.	1ncobr to npo	es, stage I	stage I–II	1f-mpo	aw	color variations from top of horizon (fine grained) to bottom of horizon (coarser-grained) faint stratified clay to gravel, some clay rip-ups >215 cm = gray (2.5YR 3/0, lake clay appearance manganese stains
Pit CS4	C	0–2	2	7.5YR 6/4-5/4	7.5YR 5/4	SL-SiL	sg-cgr	ss ps	n.o.	n.o.	n.o.	n.o.	vaw	loose silty sand in stone pavement
"post-LGM"	AvK	2–7	5	7.5YR 7/4, 7.5YR 4/6	7.5YR 6/8, 7.5YR 5/6 ped interior	SiL	3 m-c pl-abk	s p	n.o.	d, es-ev	n.o.	2f-m vesicles	aw	7.5YR 7/4-6 ped faces siltans br eff increases downward in ped interior ped interior appears more weathered than exterior
E 411197 N 6702492 7.2 m AHD	Bwkz	7–13	6	10YR 7/6	7.5YR 5/8	SL-SiL	1sg-gr	s ps	1f-cobr	d, e-ev	barely stage I	1f-m circular	cw	small blebs of salt (gypsum?)
	Btkz1	13–33	30	7.5YR 6/8	10YR 5/6	S	1sg-vf-fcr	so po	1n pf-po br	stage I, e-ev	<stage I	n.o.	di	carbonate as vf discont. coatings salt as small blebs
	Btkz2	33–65	32	7.5YR 6/8 - 10YR 10/8	10YR 5-4/6	SiL-S	1vf-fcr, 1sg gr	so po	2mk, pf-po	d-stage I, e	<stage I	1-2vf-m	vas	carbonate d to discont. coatings on clasts small blebs of salts
	2Btkz1	65–95	30	10YR 6/6 ped face	10YR 5/4	LS	2c cr f-m abk	ss po	1co-1npf	d-stage I+	d	1vf-f circular	cs	carbonate nodules up to 2 cm in diam. pockets of colloidal stains
	2Btkz2	95–145	50	10YR 7-6/8 ped face	7.5YR 5/6	SL	1sg - mf abk	ss p	1cobr-1nopo	stage1 +, ev-es	stage I	1vf-f circular	aw	carbonate nodules up to 3 cm in diam. pockets of colloidal stains siltans br <1 cm long salt xtals near base 7.5YR 5/4 crushed color
	3Btkb	145–161+	16+	5YR 5/8 ped face	5YR 4/6	SCL	cm-c-cr-1 mf sbk	ss ps	4cobr-2npfpo	d-stage I, e	n.o.	1f-vf circular	n.o.	buried soil in new parent material
Pit SC1	C	0–2	2	–	–	–	–	–	–	–	–	–	–	matrix around clasts in stone pavement
"MIS 3"	Avz	2–7	5	7.5YR 6/8	7.5YR 4/6 - 5/6	L	3 f-c abk-sbk	ss, sp	1mk silt br	n.o.	d	3 vf-f vesicles	aw	dry & wet colors from ped exterior top and interior bottom, respectively
E 414399 N 6687580 10.4 m AHD	Bwz1	7–25	7	7.5YR 5/8	7.5YR 5/6-8	L	1 sg-vf-m cr	ss ps	1n br	n.o.	d, <stage I	1vf circular	aw	small blebs of salt
	Bwz2	12–17	5	7.5YR 6-5/6	7.5YR 5/6	L	2 sg	ss sp	n.o.	n.o.	stage I to d	n.o.	ai	salt nodules up to 1 cm diameter
	Bwz3	17–22	5	7.5YR 6/8	7.5YR 5-4/6	L	sg to vf-m cr	vss vsp	n.o.	n.o.	stage I	1 vf circular	ci	salt nodules up to cm dark blebs = algae?
	Bz1	22–55	23	7.5YR 6/5-8	7.5YR 5/6 to 10YR 5/6	S	1 sg to vf-m cr	so po	1co-br	n.o.	stage I+	3 vf-m	gw	mottling banded, variable in color salt nodules up to 1 cm, 1–2 mm bands of gypsum
	Bz2	55–72	17	10YR 6/6 - 2.5Y 6/6	2.5YR 6/4	S	2sbk -vfcr	vss po	2 br	n.o.	d	3vf	gi	siltans visible wet color = 2.5Y 6/4
	Bzk	72–107	35	10YR 6/6	2.5YR 6/6 to 10YR 6/6	S	2sbk-1sg-vfcr	so po	2 br	stage I, e-es	stage I	2vf tubular to circular	cw	salt nodules & crystals up to 1 mm diameter
	Bz	107–134	27	10YR 6/6-8	10YR 6/4	S	1sg-2sbk-fcr	so po	1 br	n.o..	stage III	1f circular	aw	siltans coating clasts up to 0.5 mm thick
	2BzK	134–137+	3+	10YR 5/6, ped matrix	10YR 6/4 matrix	n.a.	1csbk-m	dry = vh	n.o.	d,e	srage IV	between xtals	n.o.	salt crystals up to 3 cm long, dominantly vertical orientation of chrystals

to redder hues (7.5YR) in the older beach ridges soils (Table 2, Figs. 3c–f), a trend also expressed in lower values in the redness index (i.e. increased redness) in the older beach ridges (Fig. 4). Despite some color variability and mottling in the Bz1–Bzk horizons in Pit SC1, reddish hues and redness are similar or slightly stronger than those of the soil horizons in the oldest landforms observed in Pit CS4 (Fig. 4). The reddest hue of 5YR was observed in the buried soil underlying the beach deposits at CS4. Generally, there are marked differences in soil color between more reddish hues and lower redness index values in the upper soil horizons (vesicular Av and/or cambic Bw horizons) and the more yellowish hues and higher index values in the lower horizons of the soil profile, respectively. In some cases, color and redness variation also coincided with stratigraphic boundaries (Fig. 4, e.g. SC5A). In profile SC5A, the Bwk horizon between 32 and 92 cm shows complex mottling with more reddish hues associated with some degree of pedogenesis in the highly irregular fingers/pockets that occurred within lighter, yellowish beach sands, and contrast with the Bqz horizons which have much more regular, horizontal boundaries (Fig. 3d). In the Avk horizon of CS4, the dry color of the interior of the Avk peds differs slightly from the exterior or ped face, reflecting slightly increased weathering in the ped interior (Anderson et al., 2002).

Pedogenic iron (Fe_d and Fe_o)

All investigated profiles exhibit a peak in pedogenic iron values (Fe_d) in the Av horizon immediately below the stone pavement. In addition they display a gradual down-profile decrease in Fe_d in the upper part of the profiles. The Holocene soil profiles (SC6A and SC5A) have significantly lower average (~0.1%) and peak Fe_d (~0.2%) values by comparison to the underlying and stratigraphically older sediments (e.g. ~0.6% at 220 cm depth in Pit SC5A) or the Pleistocene beach ridges (Fig. 4). The total values for silt and Fe_d content at SC1 are lower than those in the Pit CS4 soil profile. Among all four profiles the maximum value of ~0.8% Fe_d is measured in the Avk horizon at CS4. At this location, a secondary peak in Fe_d content occurs along with increased redness in the buried soil stratigraphically below, and truncated by, the lower beach unit (Fig. 4, Table 3). Overall, variation in Fe_d show very good correspondence to silt content. Values for Fe_o are relatively low between 0.03% and 0.3% but co-varied with Fe_d (Table 3). The Fe_o/Fe_d ratio generally shows an increase down-profile with values of ~0.4 in the upper profile and >0.8 in lower profile (Table 3). In profile SC5A, high Fe_o/Fe_d ratios in the reddish fingers/pockets of the Bwk2 deviate from the trend. Also, CS4 at Callabonna Spit is characterized by lower Fe_o/Fe_d ratio values throughout.

Carbonate ($CaCO_3$)

All profiles contain macroscopic evidence for pedogenic carbonate ($CaCO_3$) accumulation in at least one soil horizon. These range from slight effervescence to gravel clast coatings and large concretions. In addition, pedogenic carbonate content shows marked differences in overall and down-profile variation. Only very minor evidence for pedogenic carbonate was observed in the upper parts of the two Holocene profiles in the form of thin weakly developed $CaCO_3$ coatings around the larger clasts (SC6A) and slight effervescence (SC5A) in the Bwk and Bk horizons. However, disseminated carbonate and Stage I nodules were observed in the beach and lacustrine deposits below the stratigraphic boundaries in profile SC5A. In profile SC5A, however, $CaCO_3$ content, determined in the laboratory, confirmed the presence of only minor concentrations (~0.01%) in the Bwk1 and Bwk2 horizons. In SC6A peak $CaCO_3$ content (~0.9%) coincides with the Bwk not the Bk horizon (Table 3, Fig. 4). Even though the Pleistocene soil profiles CS4 and

Table 3
Results from laboratory analysis (*depths are approximate due to very irregular horizon boundaries; see text for details).

Location	Horizon	Depth [cm]	Gravel [wt.%]	Sand [wt.%]	Silt [wt.%]	Clay [wt.%]	$CaCO_3$ [wt.%]	Gypsum [wt.%]	Salt [wt.%]	pH	Fe_d [wt.%]	Fe_o [wt.%]	Fe_o/Fe_d	Bulk soil density [g/cm^3]	Hurst-Index
Pit SC6A	C	0–1	81.18	98.28	1.07	0.64	0.00	0.17	0.13	6.75	0.03	0.03	0.91	2.41	
	Av	1–2.5	15.20	76.34	16.73	6.93	0.05	0.58	0.02	6.93	0.23	0.09	0.41	1.67	17.50
	Bw1	2.5–10.5	14.02	88.93	5.83	5.25	0.05	0.35	0.01	6.98	0.14	0.06	0.43	1.81	17.50
	Bw2	10.5–23.5	14.59	93.32	2.71	3.97	0.00	0.30	0.01	7.21	0.10	0.06	0.58	1.81	12.00
	Bwk	23.5–49.5	16.88	97.24	1.22	1.54	0.89	0.13	0.01	7.41	0.04	0.03	0.65	1.83	33.33
	Bk	49.5–66.5	16.56	96.82	1.47	1.71	0.00	0.15	0.02	7.49	0.05	0.04	0.83	1.83	60.00
Pit SC5A	Av	0–3	11.33	86.56	9.11	4.33	0.00	0.37	0.01	7.12	0.18	0.05	0.28	1.75	11.67
	Bw1	3–11	7.53	90.36	6.64	3.00	0.00	0.21	0.00	6.95	0.15	0.07	0.46	1.77	11.67
	Bw2	11–32	15.25	91.55	5.14	3.30	0.00	0.17	0.01	6.91	0.14	0.05	0.36	1.82	14.00
	Bwk1	32–62*	16.62	94.97	2.70	2.33	0.01	0.23	0.03	6.81	0.08	0.04	0.47	1.83	11.67
	Bwk2	62–92*	17.80	94.02	2.45	3.53	0.01	0.41	0.09	6.95	0.09	0.08	0.84	1.83	27.50
	Bqz1	92–105	23.90	93.54	1.68	4.78	0.01	0.46	0.26	6.90	0.09	0.05	0.50	1.88	27.50
	Bqz2	105–122	19.73	91.27	2.24	6.49	0.00	0.65	0.32	7.05	0.09	0.06	0.62	1.85	30.00
	Bqz3	122–144	5.54	89.25	3.64	7.11	0.11	0.88	0.43	7.62	0.09	0.10	1.09	1.75	60.00
	2Bxk	144–179	6.96	54.49	19.14	26.38	1.22	3.89	0.97	8.30	0.25	0.19	0.76	1.45	25.00
	3Bxk	179–215	53.60	75.80	9.46	14.74	0.99	2.81	0.76	8.18	0.29	0.11	0.40	2.01	43.30
	Blk	>215	0.00	4.41	37.04	58.55	0.22	13.31	1.34	8.04	0.59	0.11	0.19	1.26	–
Pit CS4	–	0–2	24.71	66.69	23.59	9.72	0.15	1.66	0.29	8.36	0.35	0.15	0.42	1.75	21.88
	Avk	2–7	25.13	40.69	41.96	17.35	0.82	4.07	0.91	8.69	0.84	0.27	0.32	1.61	13.13
	Bwkz	7–13	18.84	59.75	28.79	11.45	0.08	9.80	2.00	7.74	0.31	0.18	0.56	1.70	10.94
	Btkz1	13–33	18.84	78.80	14.39	6.81	0.50	3.00	1.41	7.72	0.25	0.08	0.35	1.80	16.67
	Btkz2	33–65	31.13	84.36	7.92	7.71	1.22	2.41	0.60	7.81	0.35	0.13	0.36	1.90	15.00
	2Btkz1	65–95	3.59	20.27	46.88	32.85	1.06	4.36	0.94	7.96	0.31	0.16	0.52	1.34	25.00
	2Btkz2	95–145	6.19	72.13	17.08	10.78	1.22	3.52	0.71	8.12	0.29	0.08	0.29	1.61	14.58
	3Btkb	145–461	15.83	61.57	21.48	16.95	1.52	4.45	1.05	8.21	0.55	0.09	0.16	1.68	10.00
Pit SC1	A or C	0–2	–	–	–	–	–	–	–	–	–	–	–	–	–
	Avz	2–7	35.31	52.55	29.77	17.68	0.12	2.70	0.75	8.44	0.44	0.22	0.49	1.83	13.13
	Bwz1	7–12	24.42	59.23	22.01	18.76	0.05	3.34	1.65	7.76	0.39	0.19	0.49	1.74	12.50
	Bwz2	12–17	6.62	58.70	17.75	23.54	0.00	13.83	2.69	7.56	0.30	0.19	0.63	1.45	14.58
	Bwz3	17–22	19.99	64.58	18.75	16.67	0.09	3.52	2.37	7.51	0.31	0.19	0.62	1.71	13.13
	Bz1	22–55	23.63	82.58	6.25	11.17	0.05	2.89	2.03	7.39	0.18	0.11	0.61	1.84	15.63
	Bz2	55–72	29.76	66.08	21.73	12.19	0.01	3.05	1.74	7.72	0.20	0.21	1.03	1.79	18.75
	Bzk	72–107	31.47	86.25	6.33	7.42	2.38	3.93	1.52	8.02	0.15	0.13	0.86	1.90	16.50
	Bz	107–134	54.17	84.41	2.63	12.96	0.09	7.48	1.54	7.93	0.15	0.10	0.69	2.10	30.00
	2Bzk	134–137	83.63	61.31	15.94	22.75	0.47	11.23	2.45	ND	0.26	0.20	0.78	2.31	30.00

https://doi.org/10.1016/j.yqres.2014.11.002 Published online by Cambridge University Press

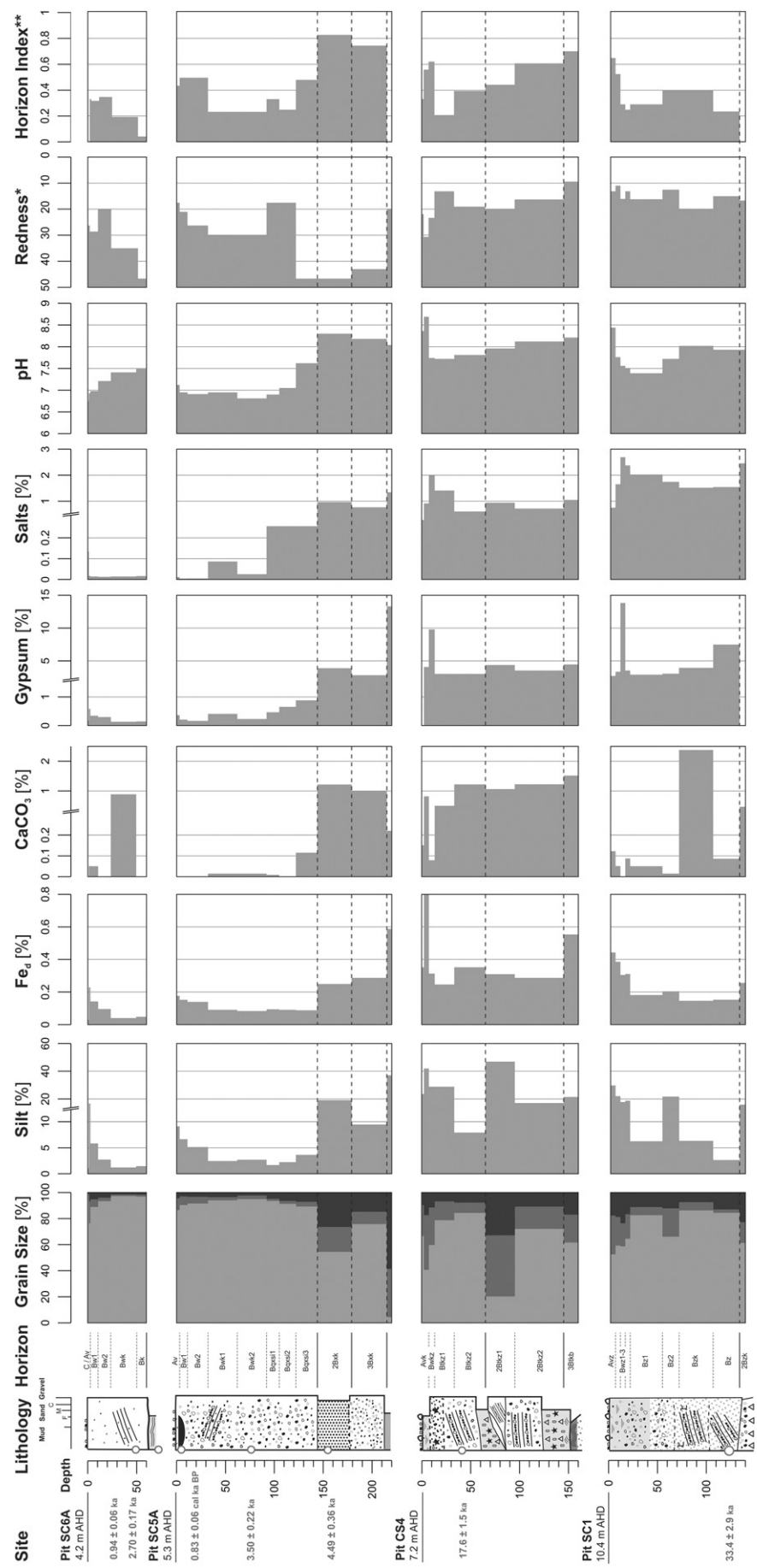

Figure 4. Lithology, stratigraphic profiles and chronology of the four studied beach ridges, and the down-profile variation in grain size, pedogenic iron, $CaCO_3$, gypsum, soluble salts, pH, Redness Rating Index (* based on Hurst, 1977), and Horizon Development Index (** based on Harden, 1982).

https://doi.org/10.1016/j.yqres.2014.11.002 Published online by Cambridge University Press

SC1 both showed two or more peaks in the down-profile $CaCO_3$ content, CS4 is characterized by significantly higher $CaCO_3$ (~1%) throughout the profile. It also contains carbonate concretions of 2–3 cm (>stage I morphology) in the 2Btkz2 horizon (note: numbers preceding letters in soil code indicate changes in stratigraphy and/or parent material). In contrast, most horizons in the oldest profile SC1 showed low $CaCO_3$ content (<0.2%) and field evidence showed only very minor macroscopic pedogenic carbonate. By contrast laboratory measurements indicated the highest $CaCO_3$ values (>2%) when compared to Bzk horizons in all studied profiles. In both Pleistocene profiles, considerable down-profile variability in $CaCO_3$ content occurs in the vesicular A (Avk and Avz) horizons and underlying cambic (Bwkz and Bwz) horizons.

Gypsum and soluble salts

All investigated profiles contain variable amounts of gypsum and soluble salts, showing good correspondence between these two components down-profile. There is a general trend of older soil profiles containing more gypsum and salts (Fig. 4). This trend is most obvious in the macroscopically observed morphology, which showed no visible accumulations of gypsum or salts in the youngest profile SC6A, some blebs and thin coatings in the mid-to-late Holocene profile SC5A, stage I blebs in profile CS4, and stage I–III blebs, bands and nodules of up to 1 cm in the oldest profile SC1. At SC1, vertically oriented gypsum crystals up to 3 cm long also occur in the 2Bzk (Table 2, Fig. 4), but most likely correspond to the lacustrine muds of an older stratigraphic unit and are thus related to non-pedogenic processes.

In general, all profiles are characterized by a peak in gypsum and salt content in the uppermost horizons within or immediately beneath the vesicular horizons. Peaks in gypsum and salt content of ~10–14% and ~2–2.7%, respectively, are significantly higher in the Pleistocene soil profiles compared to the Holocene soil profiles. Maximum values of gypsum and salts are slightly higher for the oldest soil profile (SC1) relative to the soil profile at CS4. Overall, average values of salt content are slightly higher in oldest soil (SC1), whereas average gypsum values are very similar in both Pleistocene soil profiles. In contrast to the pronounced character of gypsum peaks, however, soluble salts show a gradual decline down-profile in the soils developed on the late Pleistocene beach ridges (CS4 and SC1). Down-profile variation in gypsum and salt content in SC5A are more complex. A secondary peak occurs in the Bwk1 horizon followed by a down-profile increase towards high overall values below the stratigraphic boundaries in the lowermost profile. Additionally, in this profile prominent, centimeter-thick whitish laminations and/or drapes were observed in the Bqz1 horizon (92–105 cm). These laminations did not effervesce, do not display any macroscopic crystals form (e.g. gypsum). In addition, laboratory measurements did not determine concentrations of carbonate, gypsum or salts. Therefore these laminations are interpreted as silica accumulations.

pH values

Among all profiles, pH values are generally neutral (~7) to slightly basic (~8) but show considerable down-profile variation. In both Holocene soil profiles, pH values gradually become more basic in the lower profile. The depth of this transition varies from 10–20 cm in the youngest soil (SC6A) to ~120 cm in the mid-to-late Holocene soil profile (SC5A) (Fig. 4). In contrast, both Pleistocene soil profiles show very similar down-profile trends with maximum pH values of ~8.5 associated with the vesicular horizons in the upper most profiles followed by gradual decrease and then a renewed increase in the lower profiles (Fig. 4).

Discussion

The soil profiles exposed in the beach ridge sequence around Lake Callabonna and their associated field and laboratory data provide a unique opportunity to interpret pedogenic processes during the late Quaternary in central Australia. As the soils have formed in beach ridges that were deposited and progressively abandoned at different times ranging from MIS3 to the late Holocene, the comparison between the profiles allows for the assessment of soil development over the past ~33 ka, and its relation to landscape evolution and paleoenvironmental conditions.

Pedogenic processes in the beach ridges at Lake Callabonna

Primary sedimentary structure and properties, as well stratigraphic breaks between major depositional units, are clearly expressed at all four beach ridge sites and have not been obliterated by pedogenic processes and overprinting. There is some evidence of erosion at the boundary surfaces between stratigraphic units, especially along the lower boundaries of beach sands and gravel (e.g. CS4, SC1; Fig. 4), but there is no evidence of post-depositional erosion on the beach ridges or in the soil profiles. Even though there is minor local erosion of the beach ridges observed around Lake Frome and Callabonna, this is limited to drainage lines and small creeks that locally cut through the landforms. Overall, however there is unlikely to have been significant erosion which post-dates the onset of pedogenesis on the crests of the beach ridges. This is also reflected by the predominantly gradual down-profile changes in most soil properties (Fig. 4). In this context, the particularly well-developed pavements on the beach ridges would provide additional protection and have been shown to remain intact even through large runoff and/or sheet-flooding events (Wells and Dohrenwend, 1985). In addition, lateral displacement of clasts in the stone pavements as described by Dietze and Kleber (2012) were not observed near the study sites. As a consequence, the characteristics of the beach ridges and their associated soil profiles can be interpreted to reflect pedogenic processes and there causes.

The overall character of grain size properties on the beach ridges still reflects the differences in depositional environment between coarser, high-energy beach sands and gravel, and fine-grained near-shore lacustrine deposits (Fig. 4). Within the coarser-grained beach deposits, however, the silt and clay content varies considerably between all four profiles from ~3–11% in the Holocene ridges, to ~15–40% in the Pleistocene ridges. This could be attributed to differences in the original depositional processes and/or parent material within the high-energy beach environment, or in-situ weathering which would be expected to result in a dominance of clay over silt and a clear relationship between clay and pedogenic iron (Fe_d) from the breakdown of iron-bearing minerals. In the four investigated profiles, clay and Fe_d show a moderately weak relationship ($r^2 = 0.41$), whereas there is a stronger relationship between silt and clay content ($r^2 = 0.54$; Fig. 5b) and silt and Fe_d ($r^2 = 0.68$, Fig. 5c). Consequently, this suggests it is more likely that fines were incorporated via for example illuviation. This is strongly supported by the presence of clay and silt films (cutans/siltans) in all profiles, especially in the Pleistocene ridges. Further, the strong relationship between Fe_d and silt content throughout the four profiles also implies a common origin and pathway for Fe_d and silt, and suggests that Fe_d is not predominantly the result of the mineralogical composition of the host sediment. Iron coatings are common on eolian grains in central Australia (Bowler, 1998; Bullard and White, 2005), and may thus be incorporated into the profiles either via depositional (e.g. lacustrine) or post-depositional (i.e., pedogenic) processes.

In this context, our combined data suggest the influx and integration of eolian dust coupled with the formation of Av and Av–Bw horizons rich in gypsum and salts, implying minimal penetration of the wetting fronts on the order of few decimeters as expected in the modern arid to semi-arid environment characterizing central Australia (Yaalon and Ganor, 1973). Av horizons underlie stone pavements in all of the soil profiles observed. All Av horizons show pronounced accumulation of clay and silt of ~10–40% with gradually decreasing values lower in the profile. In contrast to desert pavements along southern Lake Eyre, which were influenced by pre-weathered silicate boulders and chemical

https://doi.org/10.1016/j.yqres.2014.11.002 Published online by Cambridge University Press

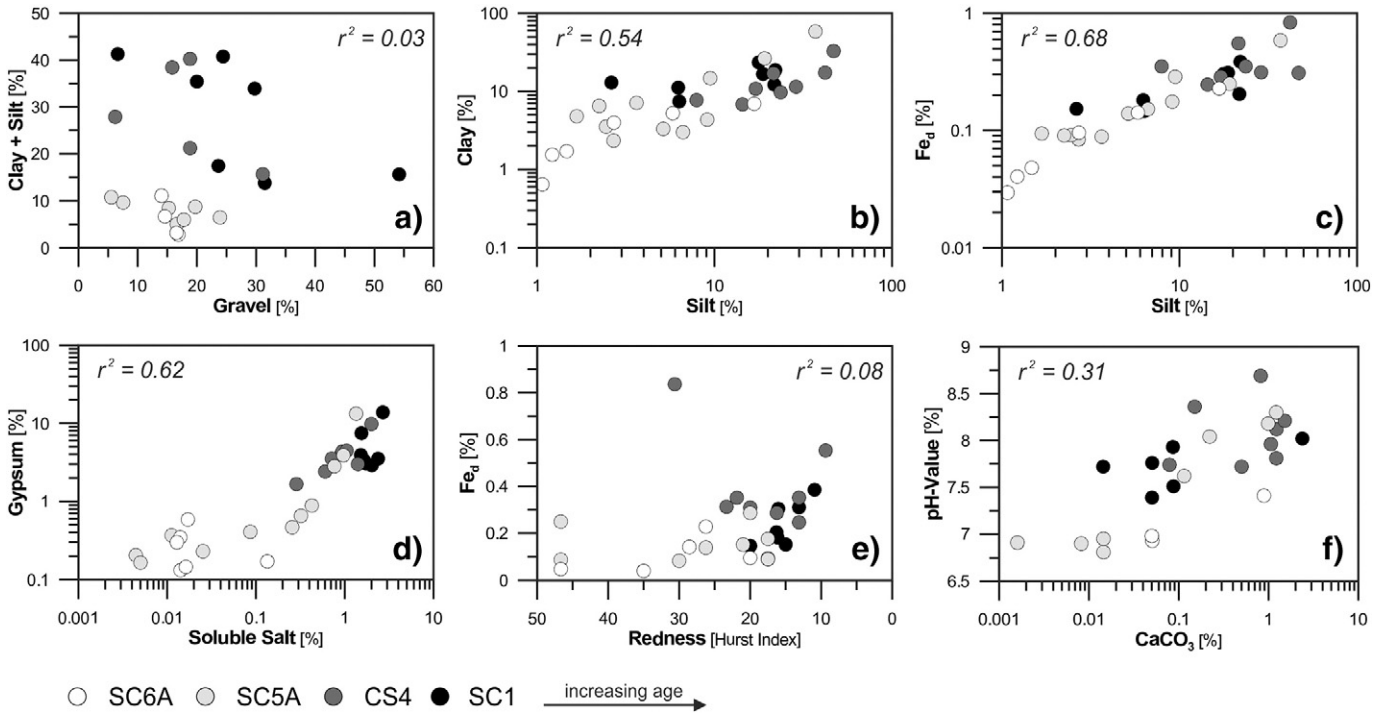

Figure 5. Relationship between selected sediment and soil parameters in all four studied profiles of increasing soil age. (a) Bulk gravel content and fines (i.e. silt + clay), (b) silt and clay content, (c) silt content and pedogenic iron Fe_d, (d) soluble salts and gypsum, (e) Redness as illustrated by the Hurst-Index (note: redness increases with decreasing values) and pedogenic iron Fe_d, and (f) carbonate ($CaCO_3$) content and pH-value.

weathering in the salt-rich environment (Al-Farraj, 2008), the formation of Av horizons in direct association with, and immediately beneath, a stone pavement is commonly associated with addition of fine-grained eolian sediment and associated iron oxides, as well as salts and carbonates derived from atmospheric and eolian sources (Wells et al., 1985; McFadden and Wells, 1987). In particular, gypsum and soluble salts show a moderate relationship ($r^2 = 0.62$; Fig. 5d), illustrating their similar pedogenic behavior and solubility. Peak values in Fe_d, gypsum and salts coincide with Av horizons in the soils formed on the Holocene ridges (Pits SC6A and SC5A). In the soils developed on the Pleistocene ridges (Pits CS4 and SC1; Fig. 4) gypsum and salt peak values are even more pronounced but are found in the cambic (or Bw) horizons below the Av horizons, suggesting the dissolution and illuviation of salt and gypsum by the wetting front into the upper soil profile, i.e. the Bw horizon. The exception to this pattern is profile SC5A, where the Bw horizons in the mid-to-late Holocene beach ridge also exhibit a peak value for red hues, apparently reflecting the increasing accumulation of iron oxides related to a thicker overlying Av horizon. Increasing redness may point to the increasing presence of pedogenic hematite as typical in warm and dry climates (Yaalon, 1979; Torrent et al., 1980, 1983; Schaetzl and Anderson, 2005) and increases with Fe_d and soil age (Figs. 3c–f), but the relationship is weak ($r^2 = 0.08$; Fig. 5e).

In all profiles macroscopic morphological evidence for secondary $CaCO_3$ at various stages of development (Gile et al., 1966) was observed in the field and clearly indicates pedogenic processes of carbonate translocation and precipitation in the soil. Down-profile variations of $CaCO_3$ values measured in the laboratory, however, differ significantly from all other soil properties, and in some cases do not match the macroscopic observations (e.g. Bwk in SC6A; Fig. 4). This suggests a more complex situation with regard to $CaCO_3$ sources, pathways, and precipitation in the four soils. Similarly, the overall relationship between pH-value and $CaCO_3$, which commonly traces the down-profile migration and distribution of carbonate and underlines the dominant effect of carbonates on soil pH, is not clear in the studied profiles ($r^2 = 0.31$; Fig. 5f). More specifically, in the Pleistocene beach ridges $CaCO_3$ content shows a gradual decrease in the uppermost profiles (e.g. Av and Bw horizons). Similar to gypsum and salts, such trends point to the incorporation of airborne (detrital) carbonate into the Av horizon, and subsequent pedogenic dissolution, translocation and re-precipitation by shallow wetting fronts. While ocean derived Ca in rain water and plant respired CO_2 has been suggested as a dominant mechanism for pedogenic carbonates in other arid settings (Quade et al., 1995; Hesse and McTainsh, 2003; Monger, 2006) sparse vegetation cover, shallow rooting depths and an almost complete absence of observed burrows or root casts, suggest that pedogenic carbonate in the studied profiles is most likely related to dissolution and re-precipitation of eolian-derived carbonates due to desiccation of the wetting front (Schaetzl and Anderson, 2005). Detailed isotopic data, however, will be required to clarify the exact relationship between carbonates and plant cover around Lake Mega-Frome.

Evolution of soils on late Quaternary beach ridges

In summary, the soil profiles on the late Quaternary beach ridges associated with Lake Mega-Frome contain evidence for a number of pedogenic processes such as the formation of desert pavements and associated vesicular horizons, the influx and translocation of eolian-derived dust into the profile, and the re-precipitation of secondary carbonate, gypsum and salts. In general, the profiles show a trend of increasing horizon development on older landforms, as with most chronosequences in arid and semi-arid regions around the world. However, the detailed nature of the soils, as reflected in the down-profile variation of soil properties, is complex, raising the question as to whether the type and intensity of the soil profiles formed in the successively older beach ridges are reflective of a mainly time dependent evolution, or potentially show the influence of other soil-forming factors.

Soil profile and horizon development

A commonly used measure for the intensity of soil development is the PDI. In the four investigated profiles PDI values are comparatively low and vary between 0.2–1.2 (Fig. 6a). As expected, PDI values for

https://doi.org/10.1016/j.yqres.2014.11.002 Published online by Cambridge University Press

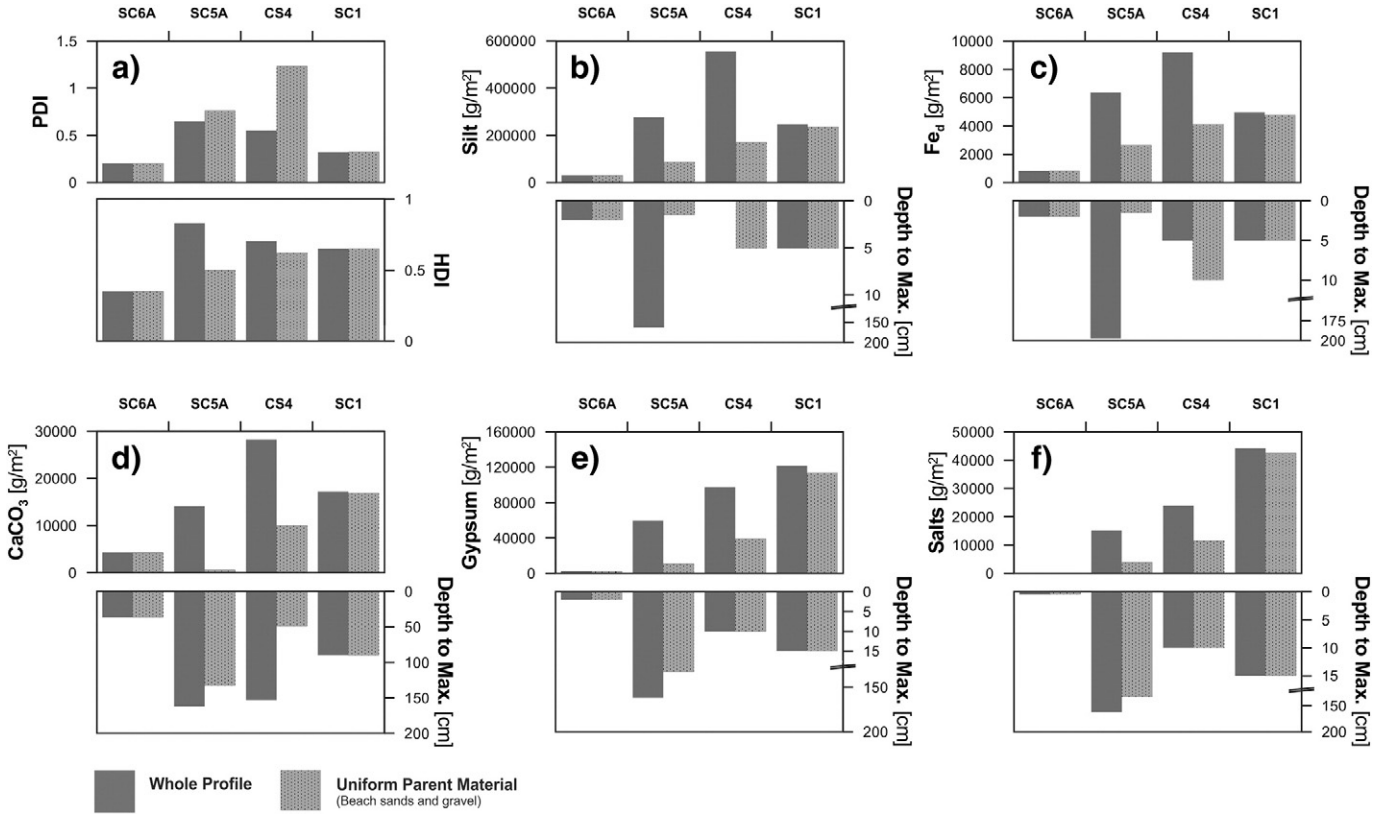

Figure 6. Summary of soil evolution with increasing soil age (from left to right) as represented by development indices (PDI and HDI), the accumulation of likely dust derived particles and chemicals (in g/m^2), and the depths to their maximum concentrations in the four studied soil profiles (in cm). Dark gray bars illustrate soil development integrating measurements over the whole profile integrating stratigraphic boundaries and differing parent material; light gray bars show soil development in the more uniform beach sands and gravel only. (a) PDI and HDI, (b) silt, (c) pedogenic iron Fe_d, (d) $CaCO_3$, (e) gypsum, and (e) soluble salts.

the four studied profiles are lower by orders of magnitude than PDI values for older soils developed in more humid regions areas elsewhere (Harden, 1982; Zielhofer et al., 2009). Even compared to soils developed in beach ridges in the semi-arid southwestern US (McFadden et al., 1992), the PDI values for the four studied profiles are much lower, implying generally weaker late Quaternary soil development around Lake Callabonna than in the hyper-arid region of the southwestern US. More importantly, the overall PDI does not show a good relation with increasing soil age as values for SC5A and CS4 are much higher than for SC6A (youngest ridge) or SC1 (oldest ridge), even if the calculation of the index is limited to soil horizons in the sedimentologically uniform beach deposits of the most recent lake stand in each pit in order to minimize the effect of differences in parent material (Fig. 6a). A similar trend is expressed by the degree of horizon development as expressed by the maximum HDI (horizon development index) value, and may imply difficulties in applying the PDI/HDI concept to soils around Lake Callabonna, particularly when considering that many of the soil morphological parameters used for quantification of the index (i.e. texture, structure, clay films as well as consistency) are related to moisture driven pedogenic processes such as clay neoformation from mineral breakdown and downward translocation, which may not always be dominant in drylands. However, a better relationship between soil properties with increasing age is reflected in the degree of horizon development (HDI) within the sedimentologically uniform deposits of the most recent lake stands. This observation highlights that variations in parent material have a strong effect on soil development, suggesting that the overall development of soil profiles at Lake Callabonna needs to be considered within the context of the sedimentological or stratigraphic framework and their vertical and lateral variations.

Site-specific vs regional-scale processes

The influence of parent material variability versus soil age on the intensity of soil development and is reflected by significant differences between the total accumulation of soil components (i.e., silt, clay, pedogenic iron, $CaCO_3$, gypsum and soluble salts) as calculated (i) for the whole soil profile (i.e. across stratigraphic boundaries and different parent sediments), and (ii) for the stratigraphically uniform coarse-grained beach deposits alone (Figs. 6b–f). Over the complete soil profile, only gypsum and salt content follow the expected trend and total volumes (i.e. weight as expressed in g/m^2) increase with soil age (Figs. 6e, f). In contrast, silt, Fe_d and $CaCO_3$ are highest in the second oldest (~17 ka; CS4) beach ridge (Figs. 6b, c, d). This may be related to the presence of a well-developed, truncated and possibly older paleosol below this beach ridge with its clearly elevated Fe_d and $CaCO_3$ content (Fig. 4). There is no apparent trend with soil age when the depth of silt, clay, pedogenic iron, $CaCO_3$, gypsum and salt maxima in the profiles are considered, likely expressing the dominant relative influence of parent material variations versus pedogenic processes (e.g. illuviation, translocation, leaching) as measured over the entire depth of the soil profiles.

When considering only that part of the soil horizons formed in uniform coarse-grained beach deposits without apparent stratigraphic breaks, all soil analyzed soil components except $CaCO_3$ exhibit a consistent trend of increasing total volumes (i.e. weights) from the youngest to the oldest soil (Fig. 6). A similar trend of increasing depth to maximum content with soil age might be interpreted for three of the investigated profiles (SC6A, CS4 and SC1). An exception to this interpretation can been seen in the soil profile at SC5A which has the overall greatest profile depths to the $CaCO_3$, gypsum, and salt maxima, and most shallow depths to silt and Fe_d content of all profiles. In addition, this soil

https://doi.org/10.1016/j.yqres.2014.11.002 Published online by Cambridge University Press

profile exhibits a marked lack of pedogenic $CaCO_3$ within the uppermost ~120 cm (Fig. 4), whereas the overall values and down-profile trend for gypsum are comparable to the youngest soil at SC6A, but are characterized by higher values for silt and Fe_d in SC5A. This implies that the mid-to-late Holocene profile (SC5A) may represent a deviation to the overall trend. Different pathways in the pedogenic evolution could be related to a high water table. A scenario of a high capillary fringe and an – at least seasonally – ascending evaporation front would agree with lake level estimates of ~3.5–4 m AHD for late Holocene lake stands (Gliganic et al., 2014), and is supported by the gradual upward decrease in the more soluble soil components such as salts, gypsum and $CaCO_3$ (Fig. 4). Very alkaline soil environments such as typical in playa-marginal settings would also lead to the salt-related modification of soil chemistry and morphology by the evaporation front (Rose et al., 2005) and could thus offer an explanation for the heterogeneous fingers and pockets as well as silica mobility in the overlying transition zone (Summerfield, 1982; Kendrick, 2007).

Influence of eolian dust

The increase in accumulated silt, Fe_d, gypsum, and salt content in the Pleistocene soil profiles (Fig. 6) in combination with the well-preserved gradual down-profile trend in these soil components within the upper profiles strongly suggest a genetic link between pavements, dust accumulation, and underlying Av horizons, requiring sufficient geologic time (Meadows et al., 2008) and implying that these pedogenic processes could have been ongoing since at least late Pleistocene in the beach ridges at Lake Callabonna. For all soil profiles except SC5A, the maxima in silt and Fe_d content as well as gypsum and salts are situated significantly deeper within the two Pleistocene soil profiles in comparison to the ~1 ka old profile (SC6A). This agrees with a scenario of the progressive development of desert pavement over time by eolian deposition and the continued translocation materials derived from these eolian sediments (McFadden et al., 1998), leading to increasing textural maturity in and immediately below the associated vesicular Av horizons. Consequently, these evolving cumulic and non-gravelly horizons additionally limit the overall rate of leaching except along abundant macropores and cracks that allow the influx of water, chemicals, and particles and further contribute to the development of the Av horizons (Anderson et al., 2002), as well as lead to bulk compositions closely reflecting simple dust and parent material mixtures (McFadden et al., 1992, 1998). The presence of gravel pavements on the surface, as well as accumulation maxima, abundant siltans and peds, and relative Fe_o/Fe_d minima in or immediately below the Av horizons, therefore together likely reflect the mechanical infiltration of eolian material and subsequent weathering processes (Anderson et al., 2002; Cornell and Schwertmann, 2006). The presence and formation of a weakly developed pavement and the accumulation of dust in the late Holocene beach ridge (e.g. SC6A; Fig. 4) implies that these processes are ongoing at Lake Callabonna and can occur over timescales of <1 ka as confirmed by other studies (Gile and Grossman, 1979; Dietze and Kleber, 2012; Dietze et al., 2012).

Implications for paleoenvironmental controls on pedogenesis around Lake Callabonna

The results of this study showed a relatively strong relationship between soil age and eolian input. However, it is important to note the results also provided evidence for the influence of soil-forming factors not related to time, such as stratigraphic heterogeneity and differences in parent material, or site-specific processes related to the topographic setting of the beach ridge in relation to other geomorphic processes. Therefore, to assess pedogenic changes over time, and discuss them within the context of sequential (time dependent) versus non-linear (climatic changes) soil development reflected in the chronosequence, average accumulation rates of silt, clay, $CaCO_3$, gypsum, salts, Fe_d and Fe_o were compared (Fig. 7). In order to minimize the effects of differences in parent material we only compare accumulation rates across the soil profiles developed within the more homogeneous beach sands and gravel. Three scenarios of accumulation were considered, each assuming slightly differing initial characteristics of the original parent material before the onset of pedogenesis (Fig. 7 for details): (#1) Beach deposits are composed of sand and gravel and were devoid of fines, measurable $CaCO_3$, gypsum, salts and pedogenic iron at the time of formation; (#2) all beach deposits contained minor initial concentrations of $CaCO_3$, gypsum, salts and pedogenic iron, equal to those found in the youngest beach ridge soil at SC6A; (#3) assumes the same conditions as scenario #2 but excludes the anomalously high $CaCO_3$ value in SC6A as it is likely derived from the presence of detrital carbonate (e.g. shell fragments). Accumulation rates vary by up to two times between these scenarios (Fig. 7). However, the general patterns are consistent between the soil profiles. It would seem unlikely that the soil profiles contain no initial $CaCO_3$, gypsum, salts and pedogenic iron given the wider environment at Lake Callabonna, consequently scenarios 2 and 3 seem more likely. These two scenarios imply accumulation rates of ~30–40 g/cm^2/yr in the Holocene profiles, and ~17–19 g/cm^2/yr in the profiles of Pleistocene age.

Although there is a paucity of dated late Quaternary dust accumulation records in central Australia (Hesse and McTainsh, 2003), the few available data indicate modern dust deposition rates of ~31–44 g/cm^2/yr (McTainsh and Lynch, 1996). Even though only a proportion of dust is generally incorporated into the soil profile (e.g. Yaalon and Ganor, 1973), these rates compare well with the accumulation rates in our Holocene profiles at Callabonna or other existing data from post-LGM soil profiles in central Australia (Cattle et al., 2002) and are moderately low in comparison with other drylands around the world (Hesse and McTainsh, 2003). At Lake Callabonna, under all scenarios the accumulation rates of silt, clay and other soil components are significantly higher in the two Holocene beach ridge soils in comparison to the Pleistocene soils. Trends in increasing Pleistocene to Holocene dust accumulation rates were also reported in the vicinity of playa lakes in the southwestern US and were interpreted with regard to changing dust generation and deposition over time (Reheis et al., 1995). Our findings may therefore suggest several possible scenarios for the late Quaternary pedogenesis as well as the generation and accumulation of dust.

During the late Pleistocene climatic conditions around Lake Frome and Callabonna are likely to have been sufficiently wet to reduce the generation of dust in the various potential source areas in southern Central Australia, e.g. floodplains, alluvial fans, and playa lake beds (McTainsh, 1989; Bullard et al., 2008). Cooler and wetter late Pleistocene conditions, at least episodically, are consistent with increased westerly derived winter precipitation. Evidence of moisture in the region at this time is provided high lake stands reflected in our studied beach ridges (Nanson et al., 1998; Cohen et al., 2012b), pollen and ostracod records extracted from lake sediments (Singh and Luly, 1991; Luly, 2001; De Deckker et al., 2011), and the formation of carbonate-rich regional paleosols around the Flinders Ranges (Williams, 1973). Increased westerly gradient winds (as opposed to southerlies and southeasterlies which currently prevail) would in addition reduce the frequency with which dust was transported to the study site (Sprigg, 1982; Shulmeister et al., 2004; Marx et al., 2011), because major dust sources, i.e. playa lakes and dune fields, are located to the east.

During the Holocene, an overall subsequent shift from positive to negative water balance conditions would have led to the present conditions of minimal leaching depths or wetting fronts, higher overall dust accumulation rates and the continued formation of desert pavements. A shift towards increased summer-dominated convectional rainfall during the Pleistocene to Holocene transition is reflected by a significant increase in grass pollen (Singh and Luly, 1991), which could have additionally enhanced the accumulation of eolian dust, as dust capturing is strongly influenced by vegetation types and density (e.g. McTainsh et al., 2002). Overall, the transition from lower Pleistocene dust input rates to higher Holocene rates could therefore be interpreted as

https://doi.org/10.1016/j.yqres.2014.11.002 Published online by Cambridge University Press

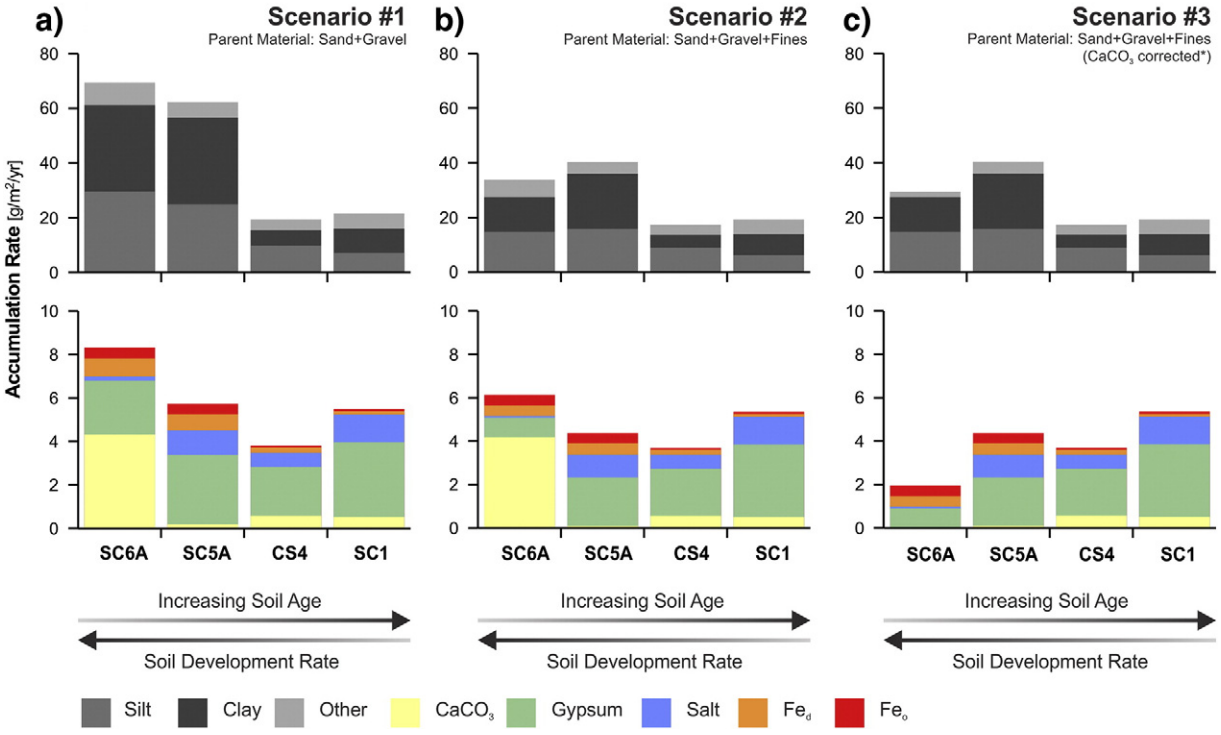

Figure 7. Summary of dust imprint on late Quaternary soil development in the coarse-grained sandy to gravelly beach deposits of a 33 ka chronosequence at Lake Callabonna as expressed by time-averaged accumulation rates in g/m^2/year for three different scenarios. The upper bar charts are estimates for total dust accumulation rates in the soil profiles detailed into silt, clay and other components; the lower charts show the varying contributions and accumulation rates of $CaCO_3$, gypsum, soluble salts, and pedogenic iron (Fe_d and Fe_o). a) Scenario #1 assumes beach deposits composed of sand and gravel, and devoid of fines and measurable amounts of $CaCO_3$, gypsum, salts or pedogenic iron. b) Scenario #2 assumes background values for fines, $CaCO_3$, gypsum, salts and pedogenic iron based on minimum values measured in the youngest beach ridge soil at SC6A. c) Scenario #3 is as #2 but accounts for anomalously high detrital $CaCO_3$ content as for example induced by the presence of shell fragments.

combination of factors which in concert resulted in reduced Pleistocene dust dynamics.

On a regional scale, reduced dust activity in the late Pleistocene seems to contradict evidence of LGM valley aggradation with reworked loessic sediments in the Flinders Ranges as suggested by Haberlah et al. (2010a, 2010b). We note however, the primary eolian deposition of the loess may have significantly predated its alluvial reworking. On a continental scale, reduced dust generation also appears to contrast marine records east of Australia, which generally indicate maximum dust activity around the LGM (Hesse, 1994; Hesse and McTainsh, 2003). On the one hand, this could suggest that overall rates in dust accumulation as expressed by the studied beach ridge soils are not representative for average conditions since the time of shoreline deposition, and might reflect a more non-linear character of pedogenesis with short and intensive periods of pedogenesis and dust accumulation followed by extended periods of relative quiescence (Huggett, 1998). However, more detailed chronological data will be required to test this scenario. On the other hand, reduced activity around Lake Callabonna during the LGM may simply be the expression of a more regional-scale response of dust activity in desert margins affected by a northward shift in westerlies, while major dust source areas in the heart of the continent may have been subjected to increased eolian activity (Marx et al., 2011; Fitzsimmons et al., 2013).

Our results indicate that average influx for clay and silt in the Holocene profiles was ~10 and 20 g/cm^2/yr. This is slightly higher than the rates reported from the southwestern US (Reheis et al., 1995). The rates deduced for the Pleistocene soil profiles at Lake Callabonna (~5–10 g/cm^2/yr) are within the range of late glacial and late Holocene rates in the Mojave desert (Reheis et al., 1995). Accumulation rates of $CaCO_3$ generally fall within the reported and highly variable range of $CaCO_3$ accumulation rates (Machette, 1985; Schlesinger, 1985; Reheis et al., 1995). In combination with the well-defined increase in silt, clay and pedogenic iron accumulation rates over the same timeframe seen in both Holocene profiles, the markedly higher $CaCO_3$ accumulation rate derived from soil profile SC6A reflects a non-eolian and/or detrital origin of the $CaCO_3$ (i.e., scenario #3; Fig. 7), implying minor $CaCO_3$ accumulation occurred in the Pleistocene and no significant $CaCO_3$ accumulation occurred in the Holocene. There was also a shift from increased gypsum and salt contributions in the Pleistocene soil profiles towards increased pedogenic iron in the latest Holocene soil profile at Pit SC6A, implying more active dust production from playa to playa-marginal sources during LGM. This inference is supported by the observation of playa derived dust in the nearby Flinders Ranges (Haberlah et al., 2010a), and the existence of ephemeral lacustrine conditions and increasing salinities in Lake Frome during the LGM (De Deckker et al., 2011). The generation of playa or playa margin derived dust would further suggest sustained sediment supply to floodplains and lacustrine systems followed by periods of desiccation and deflation of the freshly deposited material. In turn, the shift towards decreasing gypsum and salt contributions and increasing silt and iron in the dust captured in the Holocene beach ridges would point to the successive depletion of playa sources in the Lake Callabonna and Frome area due to less frequent and sustained lake events (Cohen et al., 2012b) under increasingly arid conditions. Such conditions would potentially lead to the increased derivation of eolian material from episodically active floodplains and dune fields. While this scenario would generally support the idea of the late Quaternary interplay between dust deposition rates and shifts in the westerly wind belt (Marx et al., 2011), additional research will be required to test this hypothesis.

The mid-to-late Holocene beach ridge at SC5A consists of two units of beach deposits which yielded ages of ~4.5 to 3.5 ka (Gliganic et al., 2014). This implies that the Holocene beach ridge sequences around Lake Callabonna are polycyclic in nature and may record multiple lake

https://doi.org/10.1016/j.yqres.2014.11.002 Published online by Cambridge University Press

stands (Burrough and Thomas, 2009). After 3.5 ka and the abandonment of the beach ridge at SC5A (Fig. 7), at least two additional intervals of high lake levels at ~2.7 and ~1 ka are reflected by two stacked beach units at SC6A. They likely correspond to short-lived intervals of increased precipitation (Gliganic et al., 2014) and interrupted the generally more arid and variable climatic conditions during the late Holocene (Marx et al., 2009). These lake stands and associated wet phases could be responsible for the marked pedogenic differences in the mid-to-late Holocene shorelines (e.g. Pit SC5A). Thus the combined geomorphic, chronological, and soil chemical observations for the soils exposed in Pits SC6A and SC5A appear to provide pedogenic evidence supporting the occurrence of regional late Holocene wet phases (Nanson et al., 1998; Cohen et al., 2011, 2012a, 2012b; Gliganic et al., 2014).

Conclusions

The detailed study of soil morphology and chemistry in four beach ridges of increasing age has provided the first field and laboratory assessment of a soil chronosequence formed in late Quaternary beach ridges, as well as associated pedogenic processes and possible evolutionary pathways at Lake Callabonna. The influx of eolian-derived particles and chemicals via desert pavements, their associated vesicular horizon, and shallow wetting fronts seems to exert a dominant influence on the studied soils. The successive enrichment of silt, iron, gypsum and salts is reflected by higher accumulations in the older soils, suggesting that dust incorporation and the formation of desert pavements has been ongoing since at least 33 ka. Calculated average dust accumulation rates, however, differ significantly for the Pleistocene and Holocene ridges, respectively, and may indicate climate related changes in dust dynamics and paleoenvironments. While our results imply that soils at Lake Callabonna contain valuable information with regard to pedogenesis and dust activity, they have also provided examples for their site-specific nature and the influence of parent material. In conclusion, our study suggests that soil chronosequences are powerful tools for the reconstruction of late Quaternary landscape-scale processes and paleoenvironments in the drylands of southern Australia when used carefully.

Acknowledgments

This work has been supported by funds from an ARC Discovery project (DP0667182). Gerard and Karina Sheehan of Moolawatana homestead are thanked for their hospitality and field assistance. The thoughtful comments and suggestions of David Dunkerley and Paul Hesse are gratefully acknowledged and improved the quality of an earlier manuscript.

References

Al-Farraj, A., 2008. Desert pavement development on the lake shorelines of Lake Eyre (South), South Australia. Geomorphology 100, 154–163.
Anderson, K., Wells, S., Graham, R., 2002. Pedogenesis of vesicular horizons, Cima volcanic field, Mojave Desert, California. Soil Science Society of America Journal 66, 878–887.
Barrett, L.R., 2001. A strand plain soil development sequence in Northern Michigan, USA. Catena 44, 163–186.
Birkeland, P.W., 1992. Quaternary soil chronosequences in various environments — extremely arid to humid tropical. In: Martini, I.P., Chesworth, W. (Eds.), Soils & Paleosols, Weathering, pp. 261–281.
Bowler, J.M., 1998. Willandra Lakes revisited: environmental framework for human occupation. Archaeology in Oceania 33, 120–155.
Bowler, J.M., Qi, H., Kezao, C., Head, M.J., Baoyin, Y., 1986. Radiocarbon dating of playa-lake hydrologic changes: examples from northwestern China and central Australia. Palaeogeography, Palaeoclimatology, Palaeoecology 54, 241–260.
Bullard, J.E., White, K., 2005. Dust production and the release of iron oxides resulting from the aeolian abrasion of natural dune sands. Earth Surface Processes and Landforms 30, 95–106.
Bullard, J., Baddock, M., McTainsh, G., Leys, J., 2008. Sub-basin scale dust source geomorphology detected using MODIS. Geophysical Research Letters 35, 1–6.
Burrough, S., Thomas, D., 2009. Geomorphological contributions to palaeolimnology on the African continent. Geomorphology 103, 285–298.
Callen, R.A., Tedford, R.H., 1976. New Late Cenozoic rock units and depositional environments, Lake Frome Area, South Australia. Transactions of the Royal Society of South Australia 100, 125–167.
Cattle, S.R., McTainsh, G.H., Wagner, S., 2002. Æolian dust contributions to soil of the Namoi Valley, northern NSW, Australia. Catena 47, 245–264.
Cohen, T.J., Nanson, G.C., Jansen, J.D., Jones, B.G., Jacobs, Z., Treble, P., Price, D.M., May, J.-H., Smith, a.M., Ayliffe, L.K., Hellstrom, J.C., 2011. Continental aridification and the vanishing of Australia's megalakes. Geology 39, 167–170.
Cohen, T.J., Nanson, G.C., Jansen, J.D., Gliganic, L.A., May, J.H., Larsen, J.R., Goodwin, I.D., Browning, S., Price, D.M., 2012a. A pluvial episode identified in arid Australia during the Medieval Climatic Anomaly. Quaternary Science Reviews 56, 167–171.
Cohen, T.J., Nanson, G.C., Jansen, J.D., Jones, B.G., Jacobs, Z., Larsen, J.R., May, J.-H., Treble, P., Price, D.M., Smith, A.M., 2012b. Late Quaternary mega-lakes fed by the northern and southern river systems of central Australia: varying moisture sources and increased continental aridity. Palaeogeography, Palaeoclimatology, Palaeoecology 356–357, 89–108.
Cornell, R.M., Schwertmann, U., 2006. The Iron Oxides: Structure, Properties, Reactions, Occurrences and Uses. John Wiley & Sons.
De Deckker, P., Magee, J.W., Shelley, J.M.G., 2011. Late Quaternary palaeohydrological changes in the large playa Lake Frome in central Australia, recorded from the Mg/Ca and Sr/Ca in ostracod valves and biotic remains. Journal of Arid Environments 75, 38–50.
DeVogel, S.B., Magee, J.W., Manley, W.F., Miller, G.H., 2004. A GIS-based reconstruction of late Quaternary paleohydrology: Lake Eyre, arid central Australia. Palaeogeography, Palaeoclimatology, Palaeoecology 204, 1–13.
Dietze, M., Kleber, A., 2012. Contribution of lateral processes to stone pavement formation in deserts inferred from clast orientation patterns. Geomorphology 139, 172–187.
Dietze, M., Bartel, S., Lindner, M., Kleber, A., 2012. Formation mechanisms and control factors of vesicular soil structure. Catena 99, 83–96.
Dixon, J.C., 2013. Pedogenesis with respect to geomorphology. In: Shroder, J.F. (Ed.), Treatise on Geomorphology. Academic Press, San Diego, pp. 27–43.
Draper, J.J., Jensen, A.R., 1976. The geochemistry of Lake Frome, a playa lake in South Australia. BMR Journal of Geology and Geophysics 1, 83–104.
Fedoroff, N., Courty, M.A., 1999. Soil and soil forming processes under increasing aridity. In: Singhvi, A.K., Derbyshire, E. (Eds.), Paleoenvironmental Reconstruction in Arid Lands. Oxford & IBH Publishing Co. Pvt. Ltd., New Delhi, Calcutta, pp. 73–108.
Fitzsimmons, K.E., 2007. Morphological variability in the linear dunefields of the Strzelecki and Tirari Deserts, Australia. Geomorphology 91, 146–160.
Fitzsimmons, K.E., Magee, J.W., Amos, K.J., 2009. Characterisation of aeolian sediments from the Strzelecki and Tirari Deserts, Australia: implications for reconstructing palaeoenvironmental conditions. Sedimentary Geology 218, 61–73.
Fitzsimmons, K.E., Cohen, T.J., Hesse, P.P., Jansen, J., Nanson, G.C., May, J.-H., Barrows, T.T., Haberlah, D., Hilgers, A., Kelly, T., 2013. Late Quaternary palaeoenvironmental change in the Australian drylands. Quaternary Science Reviews 74, 78–96.
Gee, G.W., Bauder, J.W., Klute, A., 1986. Particle-size analysis. Methods of soil analysis. Part 1. Physical and Mineralogical, Methods, pp. 383–411.
Gell, P.A., Bickford, S., 1996. Vegetation. In: Davies, M., Twidale, C.R., Tyler, M.J. (Eds.), Natural History of the Flinders Ranges, pp. 86–101.
Gile, L.H., Grossman, R.B., 1979. The desert project soil monograph: soils and landscapes of a desert region astride the Rio Grande Valley near Las Cruces, New Mexico. US Department of Agriculture, Soil Conservation Service, Washington, DC.
Gile, L.H., Peterson, F.F., Grossman, R.B., 1966. Morphological and genetic sequences of carbonate accumulation in desert soils. Soils Science 101, 347–360.
Gliganic, L.A., Cohen, T.J., May, J.H., Jansen, J.D., Nanson, G.C., Dosseto, a., Larsen, J.R., Aubert, M., 2014. Late-Holocene climatic variability indicated by three natural archives in arid southern Australia. The Holocene 24, 104–117.
Haberlah, D., Glasby, P., Williams, M.A.J., Hill, S.M., Williams, F., Rhodes, E.J., Gostin, V., O'Flaherty, A., Jacobsen, G.E., 2010a. 'Of droughts and flooding rains': an alluvial loess record from central South Australia spanning the last glacial cycle. Geological Society, London, Special Publications 346, 185–223.
Haberlah, D., Williams, M.A.J., Halverson, G., McTainsh, G.H., Hill, S.M., Hrstka, T., Jaime, P., Butcher, A.R., Glasby, P., 2010b. Loess and floods: high-resolution multi-proxy data of Last Glacial Maximum (LGM) slackwater deposition in the Flinders Ranges, semi-arid South Australia. Quaternary Science Reviews 29, 2673–2693.
Harden, J.W., 1982. A quantitative index of soil development from field descriptions: examples from a chronosequence in central California. Geoderma 28, 1–28.
Hesse, P.P., 1994. The record of continental dust from Australia in Tasman Sea Sediments. Quaternary Science Reviews 13, 257–272.
Hesse, P.P., McTainsh, G.H., 2003. Australian dust deposits: modern processes and the Quaternary record. Quaternary Science Reviews 22, 2007–2035.
Huggett, R.J., 1998. Soil chronosequences, soil development, and soil evolution: a critical review. Catena 32, 155–172.
Hurst, V.J., 1977. Visual estimation of iron in saprolite. Geological Society of America Bulletin 88, 174–176.
Johnson, D.L., Keller, E.A., Rockwell, T.K., 1990. Dynamic pedogenesis: new views on some key soil concepts, and a model for interpreting Quaternary soils. Quaternary Research 33, 306–319.
Kendrick, K.J., 2007. Pedogenic silica accumulation, Encyclopedia of Soil ScienceSecond edition. Taylor & Francis, pp. 1251–1253.
Lebrón, I., Herrero, J., Robinson, D., 2009. Determination of gypsum content in dryland soils exploiting the gypsum–bassanite phase change. Soil Science Society of America Journal 73, 403–411.
Leon, J.X., Cohen, T.J., 2012. An improved bathymetric model for the modern and palaeo Lake Eyre. Geomorphology 173–174, 69–79.
Luly, J.G., 2001. On the equivocal fate of Late Pleistocene Callitris Vent. (Cupressaceae) woodlands in arid South Australia. Quaternary International 83–85, 155–168.

https://doi.org/10.1016/j.yqres.2014.11.002 Published online by Cambridge University Press

Machette, M.N., 1985. Calcic soils of the Southwestern United States. GSA Special Paper 203.
Magee, J.W., Bowler, J.M., Miller, G.H., Williams, D.L.G., 1995. Stratigraphy, sedimentology, chronology and palaeohydrology of Quaternary lacustrine deposits at Madigan Gulf, Lake Eyre, South Australia. Palaeogeography, Palaeoclimatology, Palaeoecology 113.
Marx, S.K., McGowan, H.A., Kamber, B.S., 2009. Long-range dust transport from eastern Australia: a proxy for Holocene aridity and ENSO-type climate variability. Earth and Planetary Science Letters 282, 167–177.
Marx, S.K., Kamber, B.S., McGowan, H.A., Denholm, J., 2011. Holocene dust deposition rates in Australia's Murray–Darling Basin record the interplay between aridity and the position of the mid-latitude westerlies. Quaternary Science Reviews 30, 3290–3305.
McFadden, L.D., Wells, S.G., 1987. Influences of eolian and pedogenic processes on the origin and evolution of desert pavements. Geology 15, 504–508.
McFadden, L.D., Wells, S.G., Brown, W.J., Enzel, Y., 1992. Soil genesis on beach ridges of pluvial Lake Mojave: implications for Holocene lacustrine and eolian events in the Mojave Desert, Southern California. Catena 19, 77–97.
McFadden, L.D., McDonald, E.V., Wells, S.G., Anderson, K., Quade, J., Forman, S.L., 1998. The vesicular layer and carbonate collars of desert soils and pavements: formation, age and relation to climate change. Geomorphology 24, 101–145.
McTainsh, G., 1989. Quaternary aeolian dust processes and sediments in the Australian region. Quaternary Science Reviews 8, 235–253.
McTainsh, G., Lynch, A., 1996. Quantitative estimates of the effect of climate change on dust storm activity in Australia during the Last Glacial Maximum. Geomorphology 17, 263–271.
McTainsh, G.H., Love, B.M., Leys, J.F., Strong, C., 2002. Wind erodibility of arid lands in the Channel Country of western Queensland, Australia, a sequel (1994–2000). In: Lee, J.A., Zobeck, T.M. (Eds.), ICAR5/GCTE-SEN Joint conference. International Center for Arid and Semiarid Lands Studies, Texas Tech University, Texas, USA, pp. 179–183.
Meadows, D.G., Young, M.H., McDonald, E.V., 2008. Influence of relative surface age on hydraulic properties and infiltration on soils associated with desert pavements. Catena 72, 169–178.
Monger, H.C., 2006. Soil development in the Jornada Basin. In: Havstad, K.M., Huenneke, L. F., Schlesinger, W.H. (Eds.), Structure and function of a Chihuahuan Desert ecosystem: The Jornada Basin Long Term Ecological Research site. Oxford Univ. Press, New York, pp. 81–106.
Nanson, G.C., Price, D.W., 1998. Quaternary change in the Lake Eyre basin of Australia: an introduction. Palaeogeography, Palaeoclimatology, Palaeoecology 144, 235–237.
Nanson, G.C., Callen, R.A., Price, D.M., 1998. Hydroclimatic interpretation of Quaternary shorelines on South Australian playas. Palaeogeography, Palaeoclimatology, Palaeoecology 144, 281–305.
Quade, J., Chivas, A., McCulloch, M., 1995. Strontium and carbon isotope tracers and the origins of soil carbonate in South Australia and Victoria. Palaeogeography, Palaeoclimatology, Palaeoecology 113, 103–117.
Reheis, M.C., Goodmacher, J.C., Harden, J.W., McFadden, L.D., Thomas, K., Shroba, R.R., Sowers, J.M., Taylor, E.M., 1995. Quaternary soils and dust deposition in southern Nevada and California Quaternary soils and dust deposition in southern Nevada and California. Geological Society of America Bulletin 107, 1003–1022.
Rhoades, J., Sparks, D., Page, A., Helmke, P., Loeppert, R., Soltanpour, P., Tabatabai, M., Johnston, C., Sumner, M., 1996. Salinity: electrical conductivity and total dissolved solids. Methods of Soil Analysis. Part 3—Chemical Methods, pp. 417–435.
Rose, D.A., Kanukcu, F., Gowing, J.W., 2005. Effect of watertable depth on evaporation and salt accumulation from saline groundwater. Australian Journal of Soil Research 43, 565–573.
Ross, G., Wang, C., 1993. Extractable Al, Fe, Mn, and Si. Soil Sampling and Methods of Analysis 1993, pp. 239–246.
Saxton, K.E., Rawls, W.J., 2006. Soil water characteristic estimates by texture and organic matter for hydrologic solutions. Soil Science Society of America Journal 70, 1569–1578.
Schaetzl, R.J., Anderson, S., 2005. Soils: Genesis and Geomorphology. Cambridge University Press.
Schlesinger, W.H., 1985. The formation of caliche in soils of the Mojave Desert, California. Geochimica et Cosmochimica Acta 49, 57–66.
Schmid, G.L., 2013. Soil chronosequences. In: Shroder, J.F. (Ed.), Treatise on Geomorphology. Academic Press, San Diego, pp. 277–283.
Schoeneberger, P.J., Wysocki, D.A., Benham, E.C., Broderson, W.D., 2002. Field Book for Describing and Sampling Soils, Version 2.0. Natural Resources Conservation Service, National Soil Survey Center, Lincoln, NE.
Schwerdtfeger, P., Curran, E., 1996. Climate of the Flinders Ranges. In: Davies, M., Twidale, C.R., Tyler, M.J. (Eds.), Natural History of the Flinders Ranges, pp. 63–75.
Sheard, M.J., 2009. Explanatory notes for CALLABONNA 1:250.000 Geological Map, sheet SH 54-6. The Journal of the Royal College of General Practitioners.
Sherrod, L., Dunn, G., Peterson, G., Kolberg, R., 2002. Inorganic carbon analysis by modified pressure-calcimeter method. Soil Science Society of America Journal 66, 299–305.
Shulmeister, J., Goodwin, I., Renwick, J., Harle, K., Armand, L., McGlone, M.S., Cook, E., Dodson, J., Hesse, P.P., Mayewski, P., Curran, M., 2004. The Southern Hemisphere westerlies in the Australasian sector over the last glacial cycle: a synthesis. Quaternary International 118–119, 23–53.
Singh, G., 1981. Late Quaternary pollen records and seasonal palaeoclimates of Lake Frome, South Australia. Hydrobiologia 82, 419–430.
Singh, G., Luly, J., 1991. Changes in vegetation and seasonal climate since the last full glacial at Lake Frome, South Australia. Palaeogeography, Palaeoclimatology, Palaeoecology 84, 75–86.
Sprigg, R.C., 1982. Alternating wind cycles of the Quaternary era and their influences on aeolian sedimentation in and around the dune deserts of South Australia. In: Wasson, R.J. (Ed.), Australian National University, Canberra, pp. 211–240.
Summerfield, M.A., 1982. Distribution, nature and probable genesis of silcrete in arid and semi-arid southern Africa. Catena (Suppl. 1), 37–66.
Thomas, G., Sparks, D., Page, A., Helmke, P., Loeppert, R., Soltanpour, P., Tabatabai, M., Johnston, C., Sumner, M., 1996. Soil pH and soil acidity. Methods of Soil Analysis. Part 3—Chemical, Methods, pp. 475–490.
Torrent, J., Schwertmann, U., Schulze, D.G., 1980. Iron oxide mineralogy of some soils of two river terrace sequences in Spain. Geoderma 23, 191–208.
Torrent, J., Schwertmann, U., Fechter, H., Alferez, F., 1983. Quantitative relationships between soil color and hematite content. Soil Science 136, 354–358.
Ullman, W.J., Collerson, K.D., 1994. The Sr-isotope record of late quaternary hydrologic changes around Lake Frome, South Australia. Australian Journal of Earth Sciences 41, 37–45.
Wells, S.G., Dohrenwend, J.C., 1985. Relict sheetflood bed forms on late Quaternary alluvial-fan surfaces in the southwestern United States. Geology 13, 512–516.
Wells, S.G., Dohrenwend, J.C., McFadden, L.D., Turrin, B.D., Mahrer, K.D., 1985. Late Cenozoic landscape evolution on lava flow surfaces of the Cima volcanic field, Mojave Desert, California. Geological Society of America Bulletin 96, 1518–1529.
Williams, G.E., 1973. Late Quaternary piedmont sedimentation, soil formation and paleoclimates in arid Australia. Zeitschrift für Geomorphologie N. F. 17, 102–125.
Yaalon, D.H., 1979. Soils in the Mediterranean region: what makes them different? Catena 28, 157–169.
Yaalon, D., Ganor, E., 1973. The influence of dust on soils during the Quaternary. Soil Science 116, 146–155.
Zielhofer, C., Recio Espejo, J.M., Núnez Granados, M.À., Faust, D., 2009. Durations of soil formation and soil development indices in a Holocene Mediterranean floodplain. Quaternary International 209, 44–65.

https://doi.org/10.1016/j.yqres.2014.11.002 Published online by Cambridge University Press